Applied Chemical Engineering (2025) Volume 8 Issue 4 ISSN: 2578-2010 (O)
doi: 10.59429/ace.v8i4.5811

ORIGINAL RESEARCH ARTICLE

IoT-Enabled pyrolysis process system for conversion of medical plastic waste to liquid fuel as a renewable source of electricity generation

Kaushalkumar K Barot[1*], SSPM Sharma[2]

*1*Faculty of Engineering and Technology, Parul University, Waghodia, Vadodara, Gujarat, 391760, India.*
2 Department of Mechatronics Engineering, Parul Institute of technology, Faculty of Engineering and Technology, Parul University, Waghodia, Vadodara, Gujarat, 391760, India.
***Corresponding author:** Kaushalkumar K Barot; kaushal.barot@paruluniversity.ac.in

ABSTRACT

The growing volume of biomedical plastic waste, especially low-density polyethylene (LDPE) from single-use medical items, poses serious environmental and health risks due to its non-biodegradable nature and potential for contamination. Recovering energy from such waste through controlled thermal degradation processes offers a sustainable pathway to reduce pollution and generate usable energy. With the primary objective of designing and developing a waste-to-electricity generation setup using an online access tool, this research paper presents a novel setup designed and tested for receiving oil yield from a sample of low-density polyethylene plastic waste, which can be utilized for electricity generation using Pyrolysis oil. This setup has the dual benefit of waste reduction and energy production. The setup integrates IoT-based real-time monitoring through ESP32 and sensor modules to evaluate parameters such as temperature, pressure, and Pyrolytic oil yield. Data transmission is handled using the MQTT (Message Queuing Telemetry Transport) protocol and visualized via a Node-RED dashboard. Experimental trials examined the effect of process variables on oil production and energy potential. Results indicate that the optimized conditions significantly enhance oil yield, validating the feasibility of electricity generation from low-density polyethylene plastic waste. The GCV value of oil tested is 45.8 MJ/Kg. The system producing 0.19667 L/hr of pyro-oil could theoretically generate electricity 0.71 kW from medical plastic waste. This system offers an environmentally responsible alternative for energy production.

Keywords: Waste to Electricity; IoT; Pyrolysis oil; LDPE; MQTT; Node-RED

ARTICLE INFO

Received: 27 October 2025
Accepted: 2 December 2025
Available online: 10 December 2025

1. Introduction

Over the past few years, the accumulation of biomedical plastic waste has grown at a rate that has far outpaced improvements in waste management infrastructure. Much of this increase can be attributed to the global rise in the use of disposable medical supplies, particularly during and after the COVID-19 crisis. Items such as syringes, IV bags, catheters, and various forms of protective equipment are commonly manufactured using LDPE, a material prized for its flexibility and durability. However, its chemical stability and resistance to degradation make it problematic once discarded [1,2]. Medical LDPE is an almost pure hydrocarbon polymer. It improves both safety and recyclability. LDPE provides the best pyro-oil yield and energy conversion efficiency. It is one of the few medical plastics that is safe to thermally convert without producing dioxins or

corrosive gases. This process creates a way to recover resources from biomedical waste, which reduces the burden on landfills and incineration systems [3-7].

Standard biomedical waste disposal methods—both incineration and landfilling—pose serious challenges. Due to the toxic byproducts and greenhouse gases incineration produces, and the additional waste space plus the toxic leachate landfilling generates, neither of these options is sustainable, as they do not offer cleaner solutions or recover energy from the discarded material [8,9]. These issues create pressing biomedical waste disposal problems that require fuel recovery. There is a growing need to upgrade incineration practices for medical waste by using advanced emission-control systems and improved filtration technologies. At the same time, healthcare facilities must invest in cleaner, environmentally responsible methods for disinfecting and treating waste. Another important focus is the development of easily degradable materials that can be used to manufacture personal protective equipment, helping reduce long-term environmental impact [10,11]. Apart from anthropogenic activity certain biomedical waste generation methods were also conducted using bacteria through biological methods but having limitation of slow degradation rate is not applicable on large scale. However, using biological method for degradation of biomedical waste seems to be useful but needs advanced technology and took longer time in degradation as compared to pyrolysis method.

Pyrolysis, the thermal decomposition of materials in the absence of oxygen, is an example of one such solution. Decomposition of LDPE as compared to HDPE has smaller and more flexible molecular density. It is considered as bulk process of generation of carbon [12], carbon-based fabrication device [13] and moreover fuel generation from organic waste. Unlike incineration, it is capable of yielding oil, gas, or char from clothed plastics [13]. This process is especially advantageous for Low-Density Polyethylene plastics (LDPE) as it produces pyrolytic oil which contains a high energy density with low useful oil required in generators or be refined, which is why it is a substitute fuel source [14,15]. Presently many types of plastics are being used for meeting industrial requirement like polystyrene (PS), polypropylene (PP), Polyvinyl chloride and others also. As per Bell and Cave degradation of this above-mentioned plastic via natural methods using microorganism seems to be time taking and will take around 400-1000 years for complete decomposition [16]. Hence using pyrolysis for degradation of not only LDPE but effectively applied for degradation of HDPE.

By integrating the Internet of Things (IoT) in modern pyrolysis units, operators can now monitor the temperature, pressure, and oil yield, making these units much more flexible. This makes modern technologies and the rise of IoT systems a good complement to pyrolysis, which only adds to the benefits. Low-cost microcontrollers like the ESP32 can interface with cloud platforms via MQTT protocols, sending data to dashboards such as Node-RED for live visualization and control [17,18]. This level of automation allows systems to respond to fluctuations in input or environment without constant manual oversight, making them more reliable and scalable.

This study investigates the creation of a self-regulating pyrolysis system designed for biomedical LDPE waste. Our system features real-time sensors and IoT capabilities alongside a graphic interface for the remote and real-time control of the process [17,18]. We experiment to study the effect of temperature, retention duration, and feedstock on the oil yield and energy potential. The conclusions suggest a strong and efficient system capable of dealing with medical waste while recovering renewable energy and aiding the growing problem of medical waste disposal.

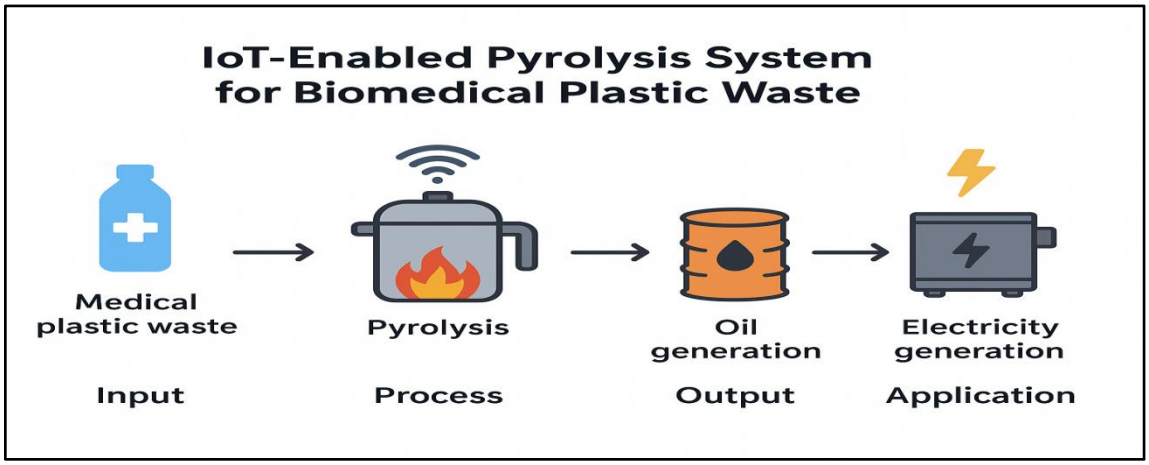

Figure 1. Waste-to-energy approach for medical plastic waste.

2. System design and methodology

2.1. Material and methods

We collected medical plastic waste of used glucose Plastic bottle scrap from small recycler firm. Discarded glucose medical plastic bottles scrap perform Sterilization, Sorting and Material Separation, washing and shredding and extrusion and pelletizing at recycler center after which medical plastic waste used as feedstock in Proposed system. The feed stock samples fed in to the reactor. The actual appearance of the medical plastic wastes weighed and added is as shown in **Figure 2**. No catalyst used in this study.

The pyrolysis experiment was conducted in the block type batch reactor made of SS 316 covered with outer insulation. The inside diameter and height of the pyrolyzer were 202 mm and 325 mm. The reaction temperature in the pyrolyzer was controlled with K-type thermocouple and heater. A Vertical Shell and Coil Condenser E 0.21 M^2 and E 0.12 M^2 connected to outlet of the reactor to condense liquid. Liquid product and solid residue were collected and weighted.

Figure 2. Medical plastic waste feed stock weighted and added in reactor.

In the experiment used 2 kg of the feed stock of medical plastic waste material fed into the reactor. the reactor heated from room temperature to the targeted temperature. The biomedical plastic waste was then melted and volatized into the condenser. The thermal pyrolysis experiments were carried out at the reactor temperature 180 ºC, 200 ºC and 250 ºC. The HHV of the liquid sample measured using Bomb calorimeter. The faction of liquid product was also analyzed by using GC-MS (Autosystem XL GC with Turbomass).

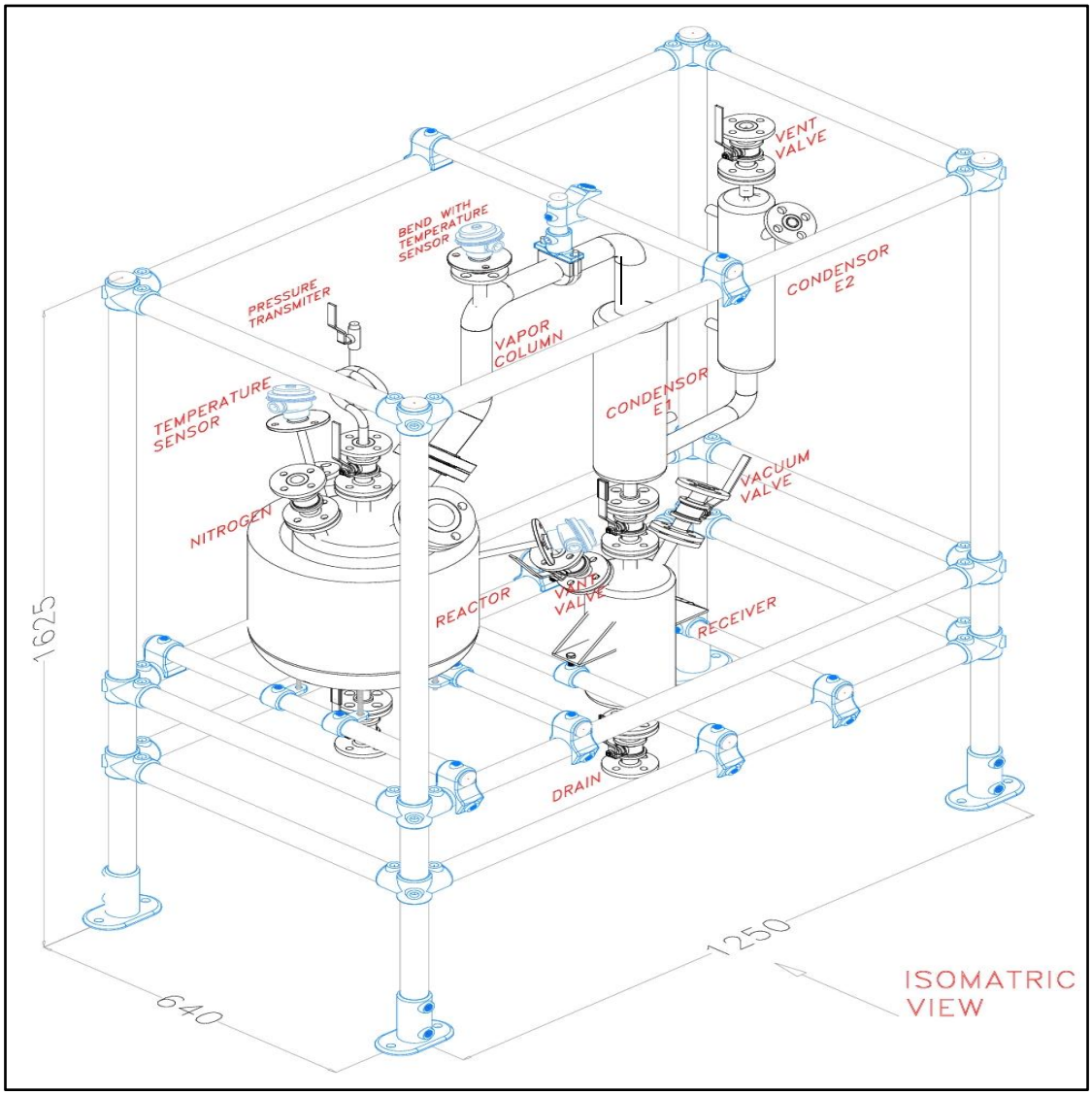

Figure 3. CAD model of the experimental apparatus.

2.2 Mechanical design

2.2.1 Five liter pyrolysis system

Apparatus made of SS 316 material with Operating Process Temperature value up to 500°C with 6 bar operating pressure with 5 L of capacity in which block type heater is used with outer side insulation with capacity of 3.3 kW. We have design for single phase supply. Set up equipped with load cell for automatic liquid measurement and display.

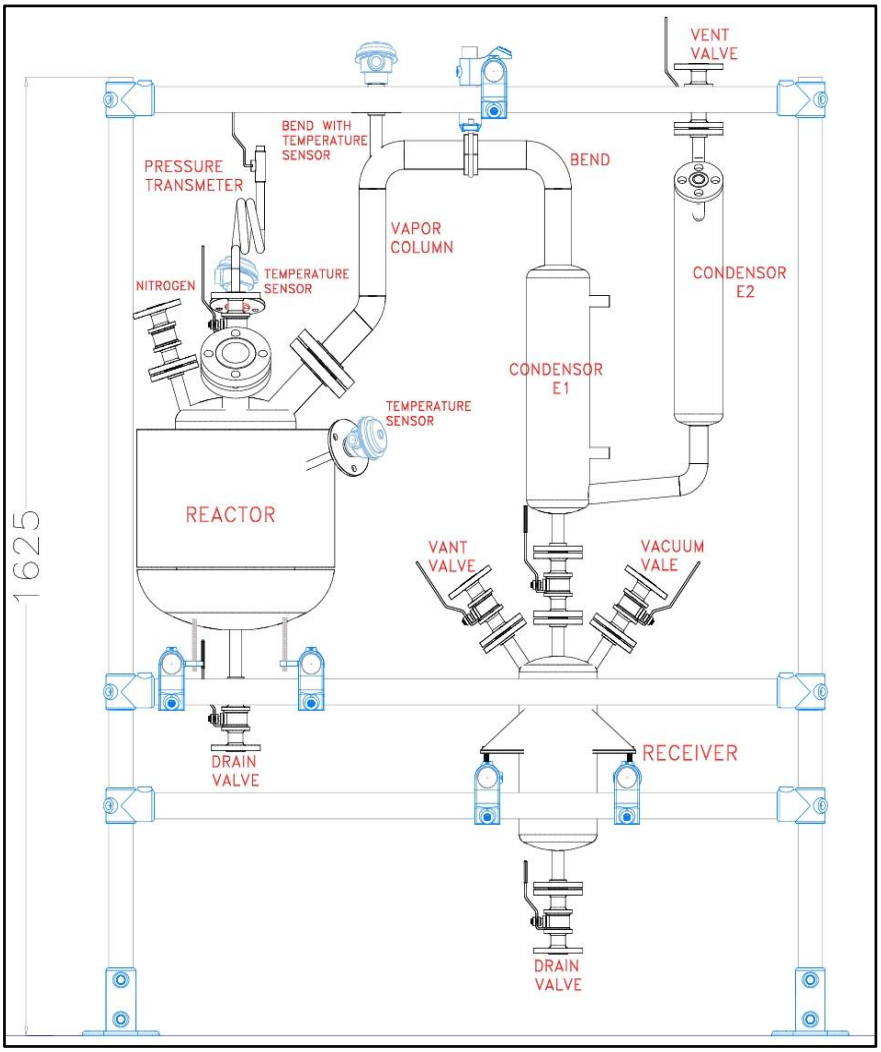

Figure 4. A schematic diagram of 5-liter pyrolysis system.

2.2.2. Five-liter reactor design

LDPE material density:925 to 940 kg/m³

Outside Diameter:219.1 mm

In side Diameter:202.7 mm

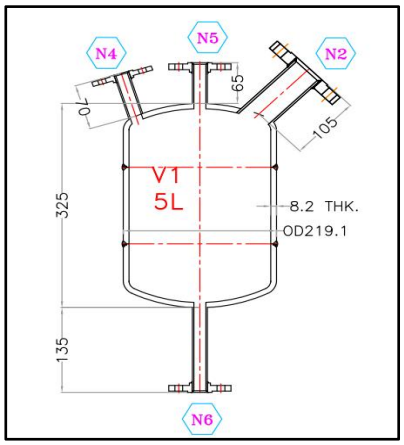

Figure 5. A schematic diagram of 5-liter reactor.

Thickness:8.2 mm

Volume of Reactor:0.005 m^3

Condenser Length:329 m

Surface area of cylinder:2*3.14*r*h+2*3.14*r*r

=0.298959 m^2

As per ANSI B16.9 PIPE OD and wall thickness and welding fittings.

The proposed system offers a new IoT-enabled pyrolysis reactor designed for medical-grade LDPE. It includes precise zonal heating heater power is adjusted by automated PID control to maintain the ideal temperature for LDPE cracking with uniform thermal distribution, and improved condensation for LDPE vapors. Additionally, it features real-time adaptive control.

2.2.3. Liter storage reactor design

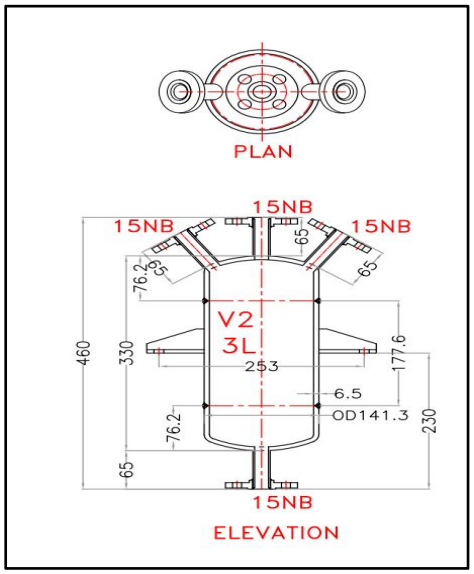

Figure 6. A schematic diagram of 5-liter reactor.

LDPE material density:925 to 940 kg/m^3

Outside Diameter:141.3mm

In side Diameter:128.3 mm

Thickness:6.5 mm

Volume of Reactor:0.003 m^3

Surface area of cylinder:2*3.14*r*h+2*3.14*r*r

=0.146485 m^2

2.2.4. Condenser unit design

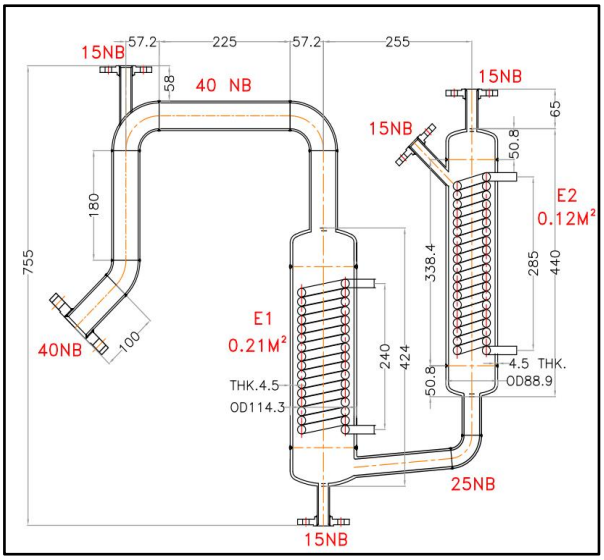

Figure 7. A schematic diagram of condenser design.

One turn Length=3.14*D

=3.14*89

=279.46 mm

For 17 turns=17*279.46=4750 mm

E1=3.14*0.014*4.75=0.21m²

Similarly for 0.12 m²

2.2.5. Heater selection

Power :3.3 kW (Ceramic type Band heater), Inside Diameter of Reactor: 270 mm, Height:230 mm

Figure 8. Ceramic type Band Heater

Area= 270 * 230 mm² = 62100 mm²= 96.19 In², 3366.65 Watt =3.3 kW, Operating Voltage:230 V

Maximum Voltage: 230 V +/- 5 %, Operating Current: 16 A, Maximum Current: 20 A.

2.2.6. Hydro test of WTE sdystem

A hydrotest test, is a process for detecting leaks and structural weaknesses in a WTE system by filling it with water and pressurizing it. Fill the vessel with water. The water may be dyed to help with visual leak

detection. Seal the ends of the reactor. Connect a pump and pressure gauge. Pressurize: Pressurize the vessel or pipe to 1.5 times its design pressure. (30 to 50 bar as per ASME B31).

Figure 9. Hydro Test of WTE Setup

Monitor the pressure for a set period of time. If the pressure drops, it indicates a leak. Check for any leakage or damage.

2.3. IoT system design

2.3.1. Panel connection diagram

Panel Diagram Consist of Two temperature indicator module UT 38 with built in RTD (Resistor temperature Detector) Sensor PT-100, Pressure Indicator PI 38, PID controller, Solid state relays, Motor etc.

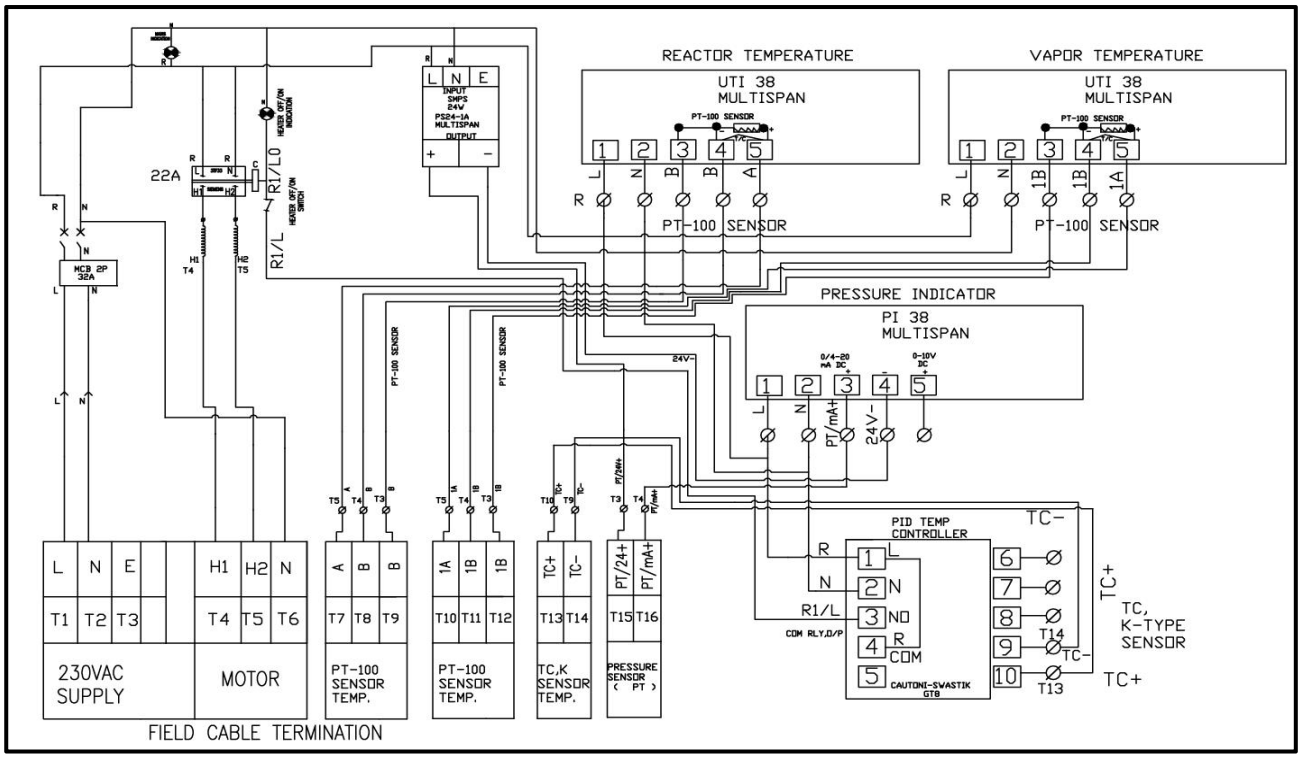

Figure 10. Panel Connection Diagram

PID controller will detect the temperature and pressure variations from the input and it control the output proportion to the variations of Inputs. Motor is used for water circulation inside condenser to convert vapor to liquid form 24 Volt SMPS provides the DC power supply to the overall circuit. In this Panel Diagram initial testing executed with PT 100.

2.3.2. Identification of Iot requirement

Microcontroller ESP 32 is required for connecting the device to cloud and stored data. Esp 32 fetches the data of temperature sensor from PID controller. Free Cloud required to share the data. Weight of the liquid is also measured and displayed in cloud using weight sensor Load Cell connected to microcontroller.

System Block Diagram:

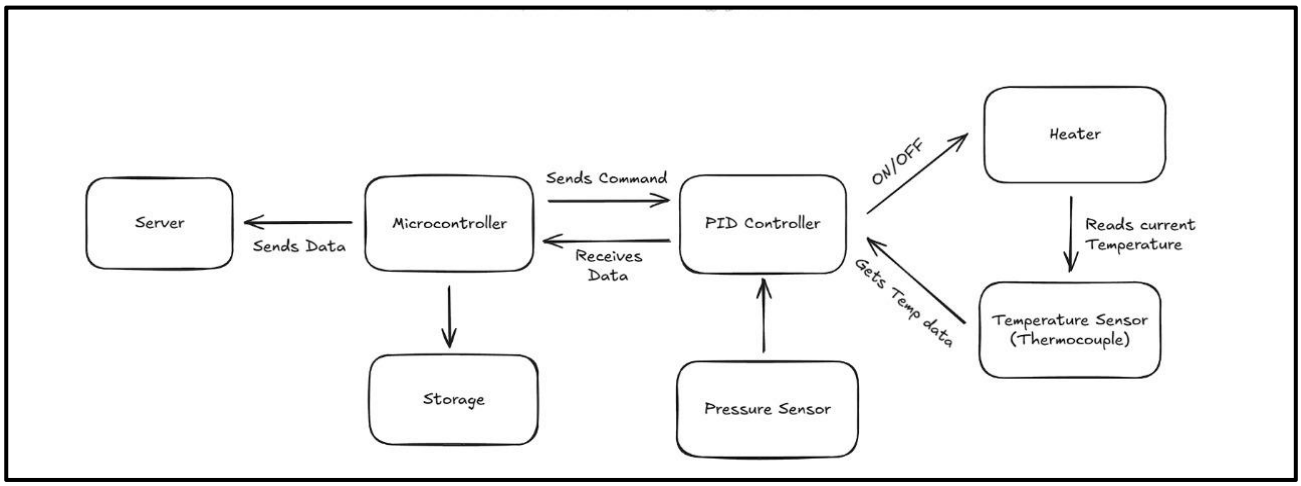

Figure 11. System Block Diagram.

ESP 32 works on 5-volt DC. ESP 32 communicates with the PID controller through UART toRS485 converter. With the help of this communication the ESP32 can set the temperature and get the current temperature. The PID controller works on 230 volts AC The PID controller turns on the heater through a SSR depending on the current and set temperature. The load cell works on 5-volt DC. The load cell is connected to ESP32 through I2C communication. The load cell is used to determine the weight of the output liquid. The pressure sensor module works on 5-volt DC. The output of pressure sensor module is analog voltage so it is connected to the analog pin of ESP32. ESP32 can read the voltage on this analog pin and find the pressure.

ESP32 is used as Main MCU to control the Process. Project includes different modules such as Temperature Indicator UTI 38, Solid State Relay SSR, PID controller, Heating Element for the Heater, Pressure Indicator PI 38. Built in Temperature indicator UTI 38 is used to read and display the temperature variation. Resistor Temp Detector PT 100 (temperature sensor) used to read temperature value from -200 degree to 850 degree.PID Controller which control the Heater element based on the Temperature variation. PID Controller is connected through Solid State Relay (SSR) to control the Turn ON and Turn OFF the Heater. Display unit will display all the Temperature and Pressure variation. Sensor Used for reading the temperature is RTD PT100.Electric Contactor is used to connect all electric connection to all devices.

2.3.3. Circuit diagram

ESP 32 Shield is used as microcontroller for controlling the device. Hardware simulation uses Temperature sensor PT 100, Load Cell, ADC module, AC Heater through SSR, Solenoid valves switching through relays are connected with microcontroller (ESP32). Temperature variations will be reading and deployed into cloud through Wi-Fi using Temperature sensor PT100.

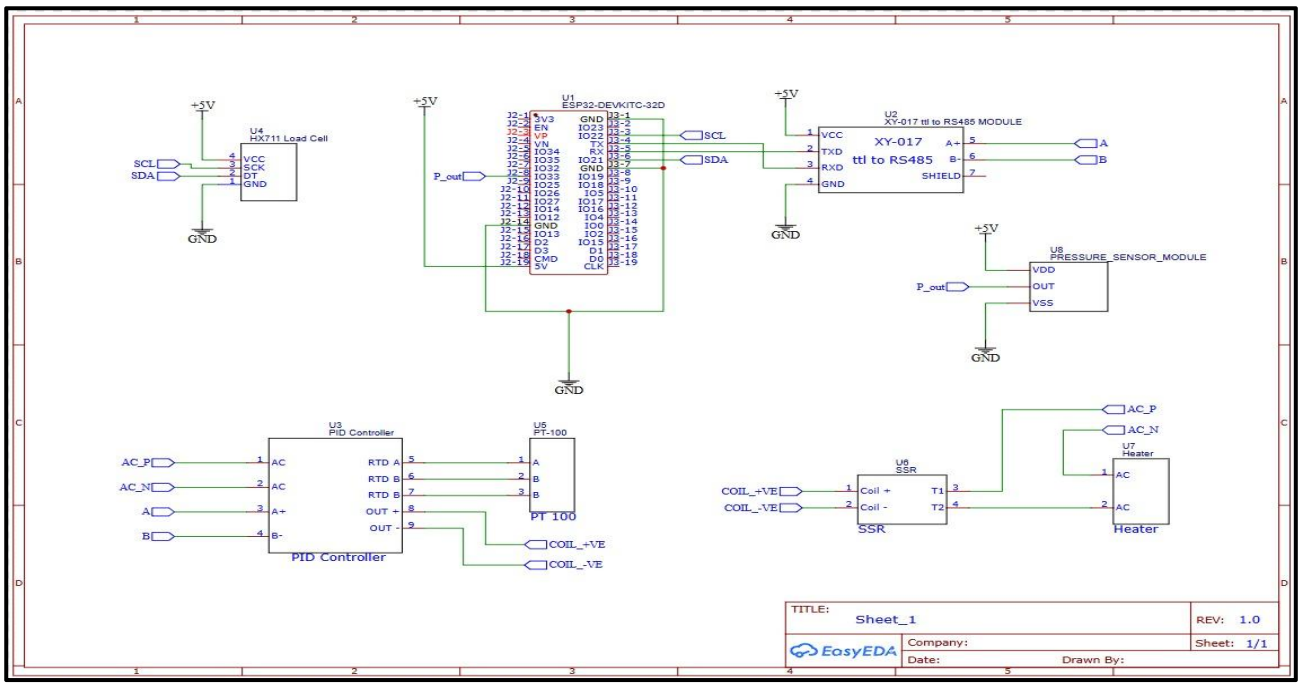

Figure 12. Circuit Diagram

AC Heater will be operated with the help of PID controller and connected with SSR. Weight of the liquid is measured by Load cell and converted to digital data and given to microcontroller for storing in Cloud. Solenoid Valves are operated through relays based on the conditions written in the program.

2.3.4. Sensor integration and cloud integration

1) Temperature Sensing: RTD PT100 feeds data to PID Controller.PID sends processed data to ESP32.

2) Weight Sensing: Load Cell measures liquid output weight. Connected via I2C communication to ESP32.

3) Pressure Sensing: Analog Pressure Sensor to ESP32 Analog Pin. Real-time pressure monitoring.

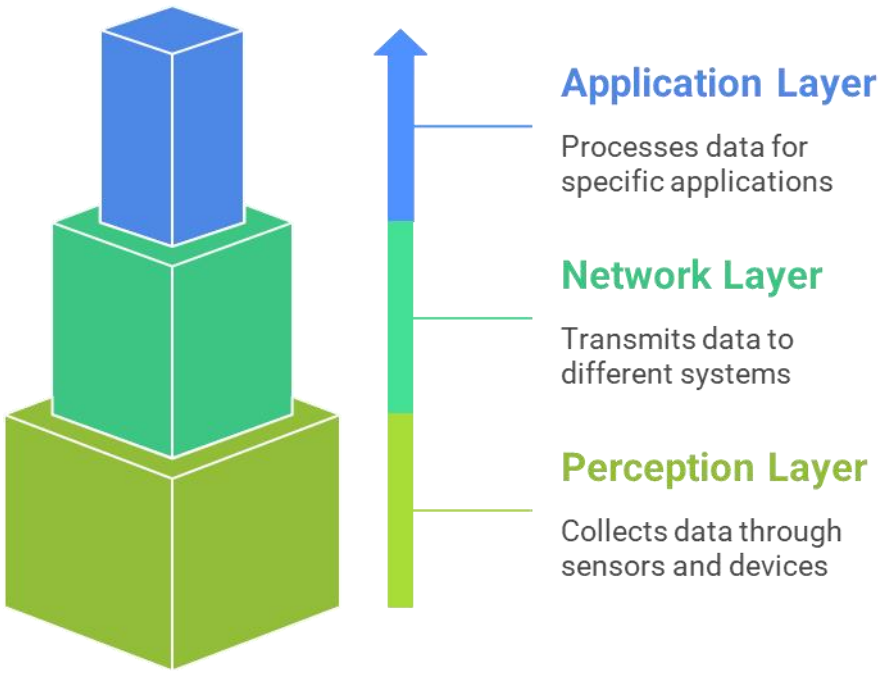

Figure 13. IoT 3 Layers Reference Model

2.3.5. Simulation steps

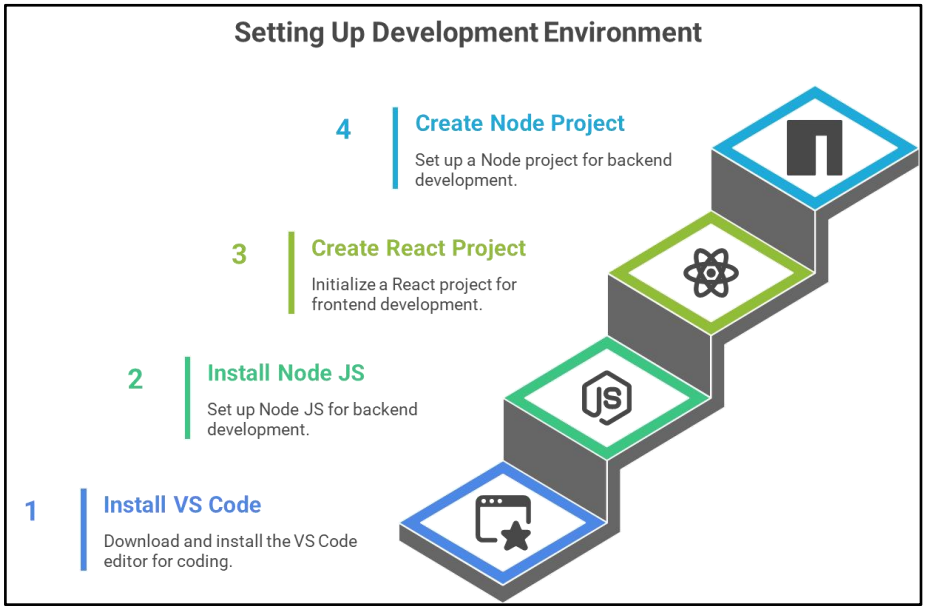

Figure 14. IoT 3 Layers Reference Model

STEP-1: Installing VS code Editor

https://www.c-sharpcorner.com/article/how-to-install-visual-studio-code-on-windows-11/

STEP-2: Installing Node JS

https://kinsta.com/blog/how-to-install-node-js/

STEP-3: Creating A React Project (Frontend)

https://www.c-sharpcorner.com/article/create-a-react-app-in-the-vscode/

STEP-4: Creating A Node Project (Backend)

https://aunsh.medium.com/initialize-a-project-in-node-with-npm-init-dc6f2196033

2.3.6. Circuit module

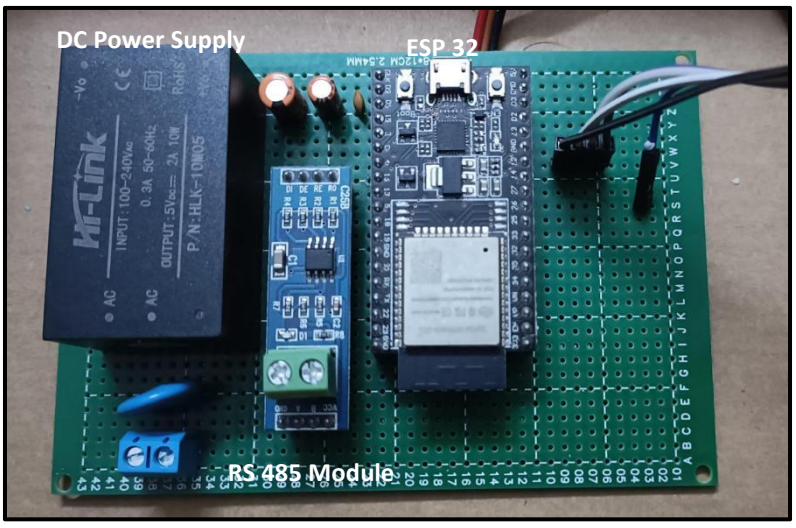

Figure 15. The Final system of IoT

ESP 32 works on 5-volt DC. ESP 32 communicates with the PID controller through UART toRS485 converter. With the help of this communication the ESP32 can set the temperature and get the current temperature. The PID controller works on 230 volts AC The PID controller turns on the heater through a SSR depending on the current and set temperature. The load cell works on 5-volt DC. The load cell is connected to ESP32 through I2C communication. The load cell is used to determine the weight of the output liquid. The pressure sensor module works on 5-volt DC. The output of pressure sensor module is analog voltage so it is connected to the analog pin of ESP32. ESP32 can read the voltage on this analog pin and find the pressure.

Table 1. Main active components of the board.

Modules	Amount	Modes	Current Capacity (µA)	Operating Voltage (V)	Power (W)	Total Power	Running Time (s)	Prices ($)
ESP32	1	On	80,000	5	0.4	0.4	3600	6.0
MAX485 TTL to RS485	1	On	120	5	0.6	0.6	3600	1.5
Load Cell 5KG	1	On	10	5	0.05	0.05	3600	5.0
SRF-05	1	On	4	5	0.02	0.02	3600	3.0

2.3.7. Illustration of the overall IoT system

The Node System Connected to the cloud Fire base through Server. Data Generated from Node with Set value will be storing to Cloud. The Web Page Application (API) Is designed to plot the real time and set value. API is Interface through Cloud and Exchange the Data.

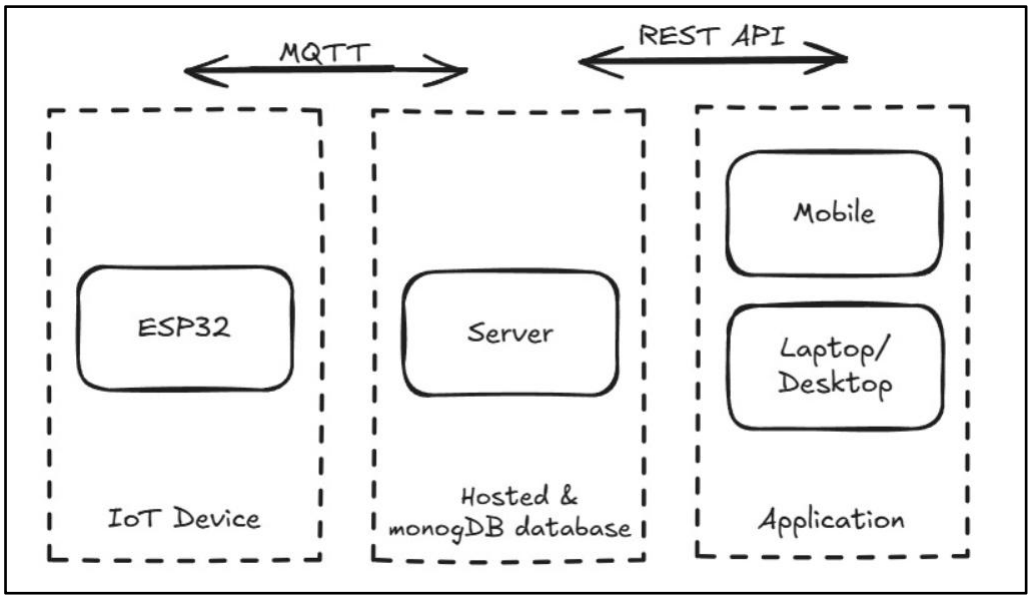

Figure 16. Subsystems that form the connection of the IoT node with the application

2.3.8. Data monitoring and analytics

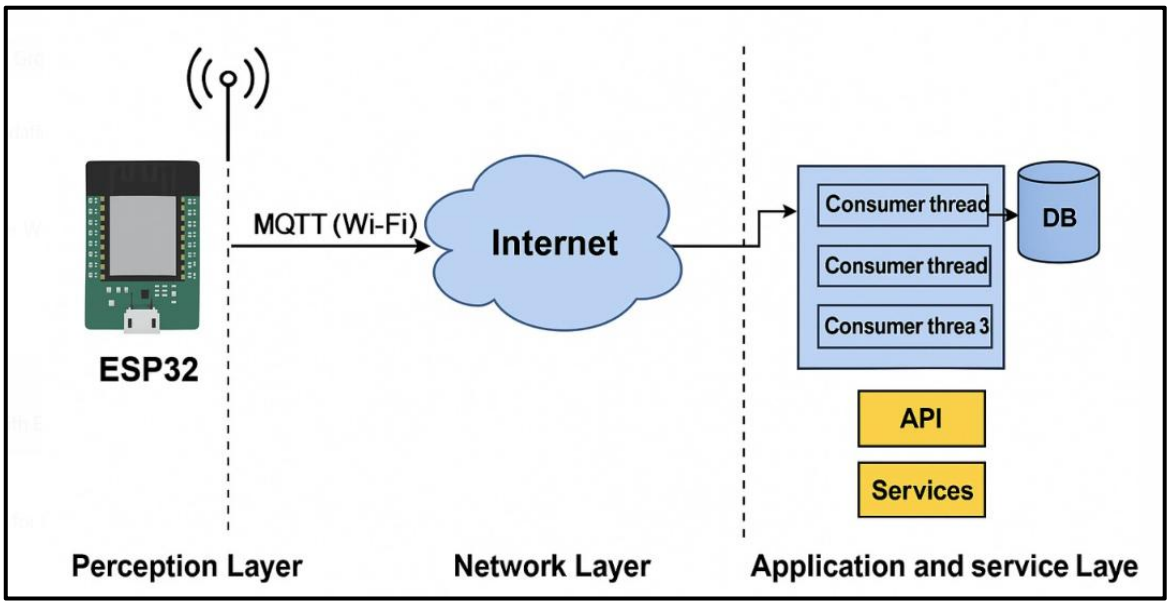

Figure 17. Data monitoring and analytics

From the above Model data generated from node sent to cloud through Gateway. Set point can be set from API (Application Programme Interface) designed Webpage. Data will be saved in Cloud (Mongo DB). Fire base Protocol used for storing Data to Cloud.

The enhanced monitoring setup brings together data from multiple sensors, live IoT connectivity, smart PID-based control, built-in safety prediction, and cloud-level analytics. This combination allows the system to run the pyrolysis of high-purity medical LDPE with far greater accuracy, stability, and efficiency than what is possible in traditional pyrolysis units.

2.3.9. Data exchange and methodology

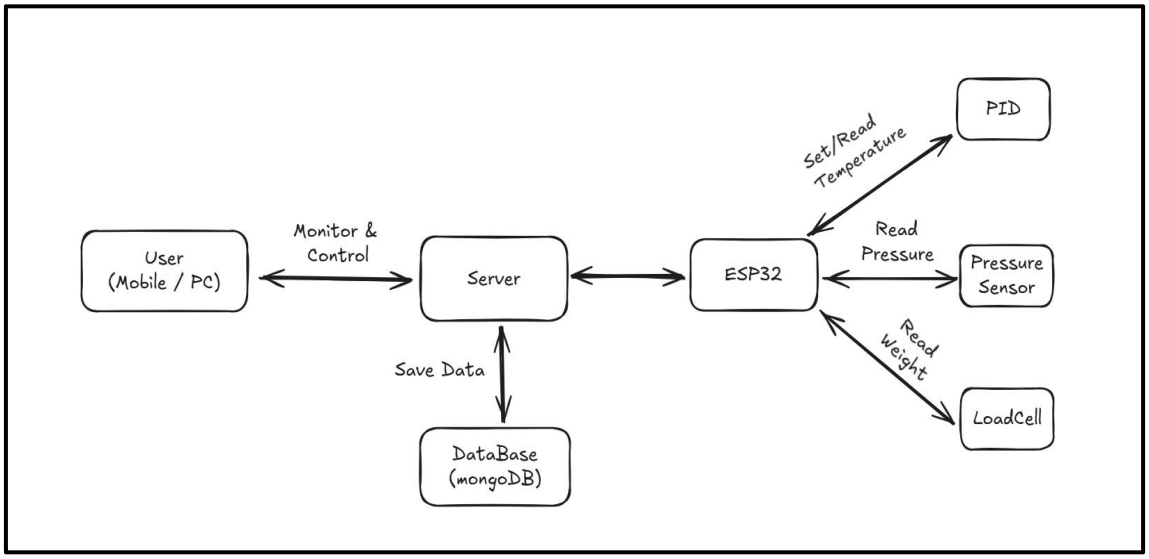

Figure 18. Data Exchange

The proposed methodology for the present study is as, follows:

(1) Set the Temperature & Start the heating using Web User Interface.

(2) ESP Monitors Temperature, Pressure, Weight and sends it to the Server.

(3) Server saves the data in the Database.

(4) User Can monitor the Live Data and also view the Report.

3. Results and discussion

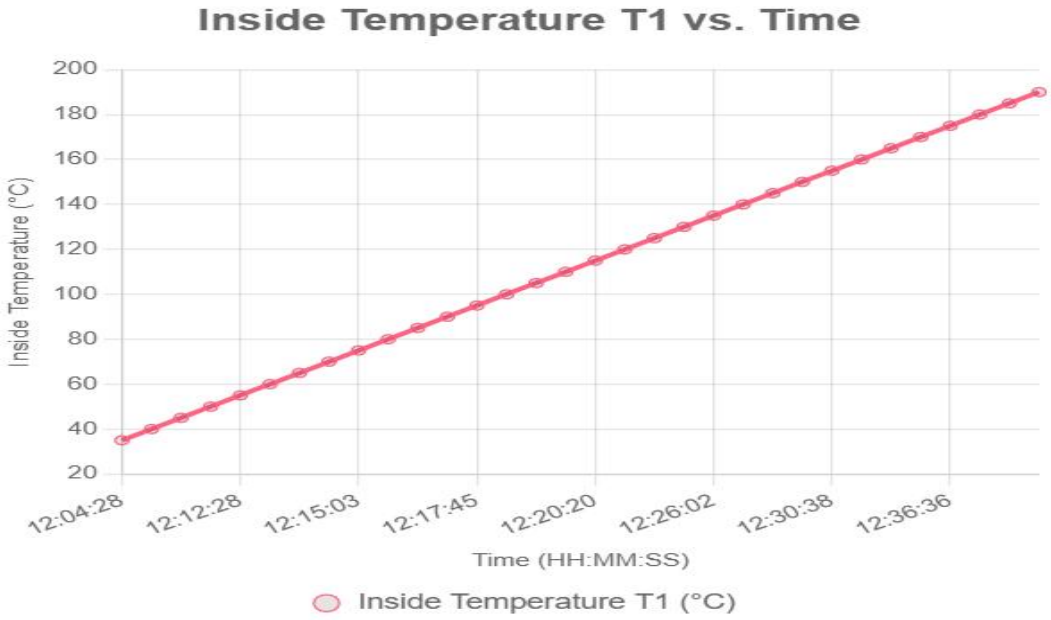

Figure 19. Inside Temperature Vs Time

The inside temperature (T1) exhibits a linear increase from 35 °C at 12:04:28 to 190 °C at 12:42:01 over approximately 37.55 minutes. The rate of increase is consistent, averaging ~4.1 °C/min, indicating a steady heating process within the system. No fluctuations or plateaus are observed, suggesting stable thermal input.

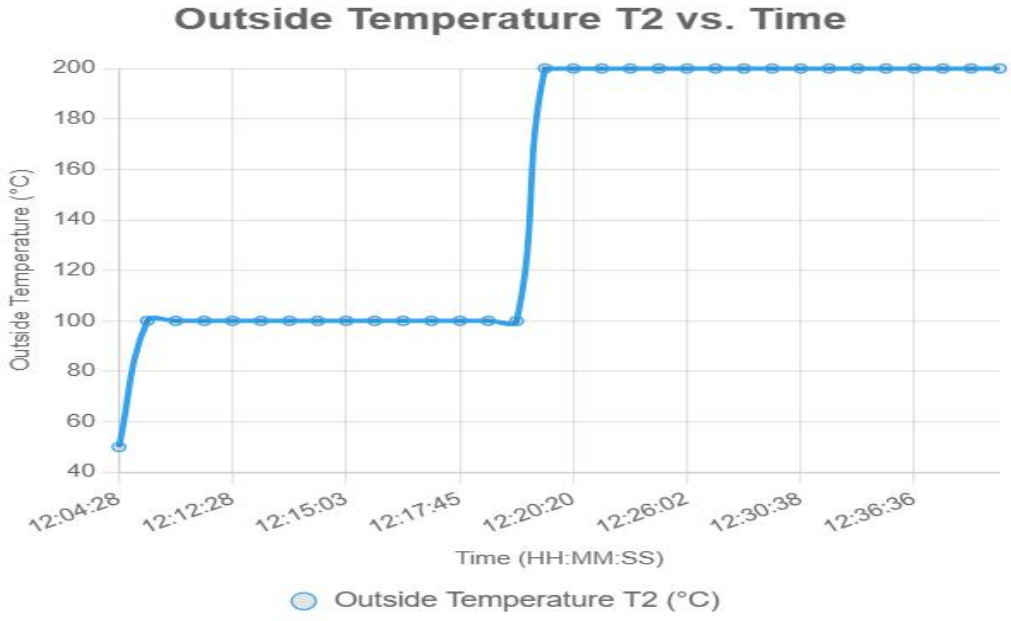

Figure 20. Outside Temperature Vs Time

The outside temperature (T2) shows a step-wise increase, starting at 50 °C (12:04:28), rising to 100 °C by 12:09:37, maintaining 100 °C until 12:18:34, then jumping to 200 °C at 12:19:23 and remaining constant

thereafter. The abrupt transitions suggest controlled external temperature changes, possibly due to environmental or equipment adjustments, with no gradual variations.

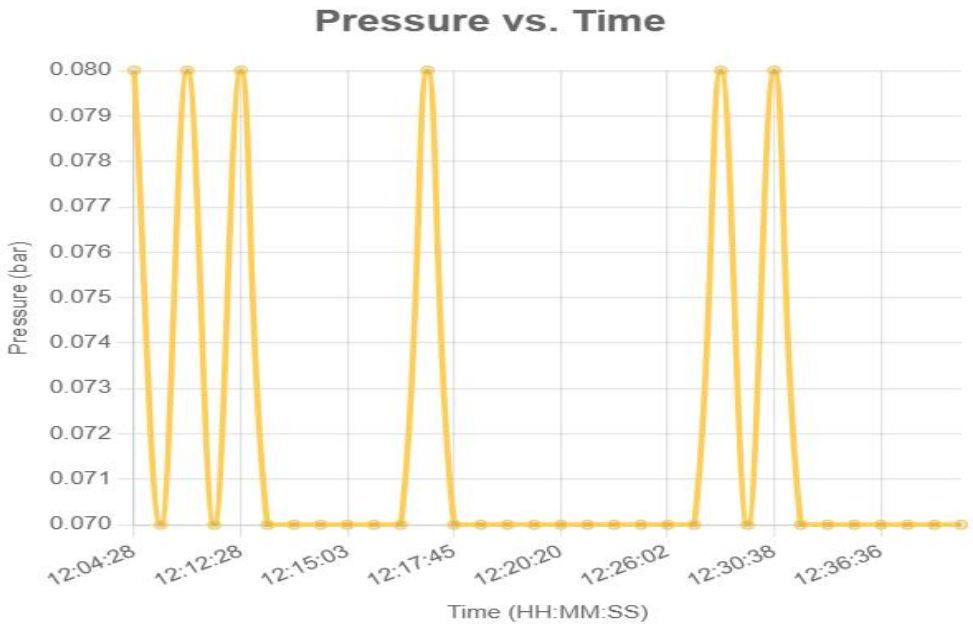

Figure 21. Pressure Vs Time

Pressure remains nearly constant, fluctuating narrowly between 0.07 and 0.08 bar from 12:04:28 to 12:42:01. The mean pressure is ~0.071 bar, with minor oscillations (±0.01 bar) at specific points (e.g., 12:04:28, 12:12:28, 12:28:20). This stability indicates a well-regulated system with minimal pressure dynamics during the observed period.

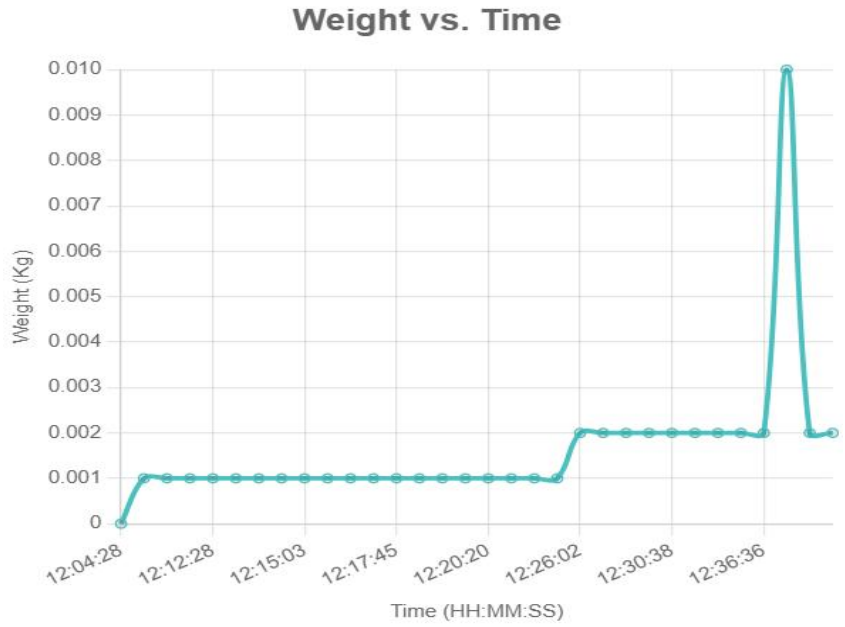

Figure 22. Weight Vs Time

Weight increases slightly from 0.000 Kg at 12:04:28 to 0.001 Kg by 12:09:37, remains at 0.001 Kg until 12:24:41, then rises to 0.002 Kg at 12:26:02, maintaining 0.002 Kg thereafter, except for a capped peak of 0.01 Kg at 12:38:06 (originally 0.0141 Kg). The overall trend suggests a gradual mass accumulation, with the capped outlier indicating a possible transient event or measurement anomaly.

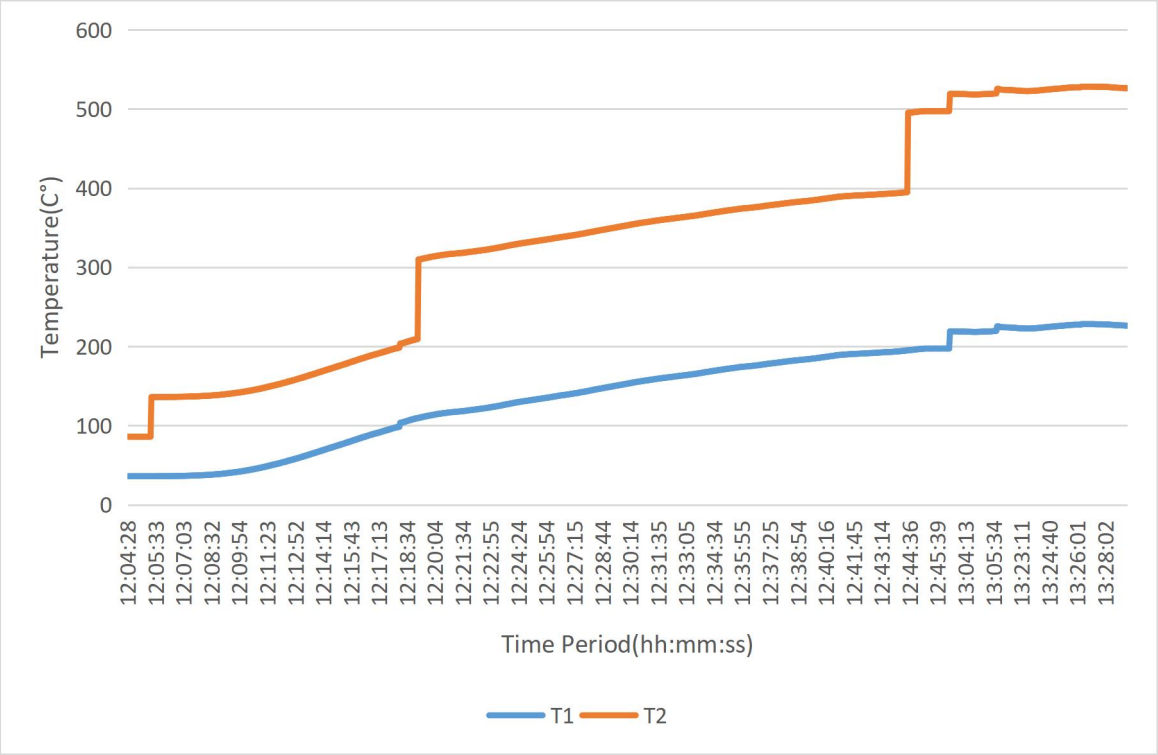

Figure 23. Temperature Vs Time

Both T1 (blue line) and T2 (red line) show a general increasing trend over time. T1 rises steadily and more gradually. The final temperature of T2 is over 500°C, while T1 reaches just over 220°C, indicating a large temperature gradient between the two. The X-axis shows a continuous time period, indicating the heating process took around 1 hour and 25 minutes, from approximately 12:04:28 to 13:28:02.

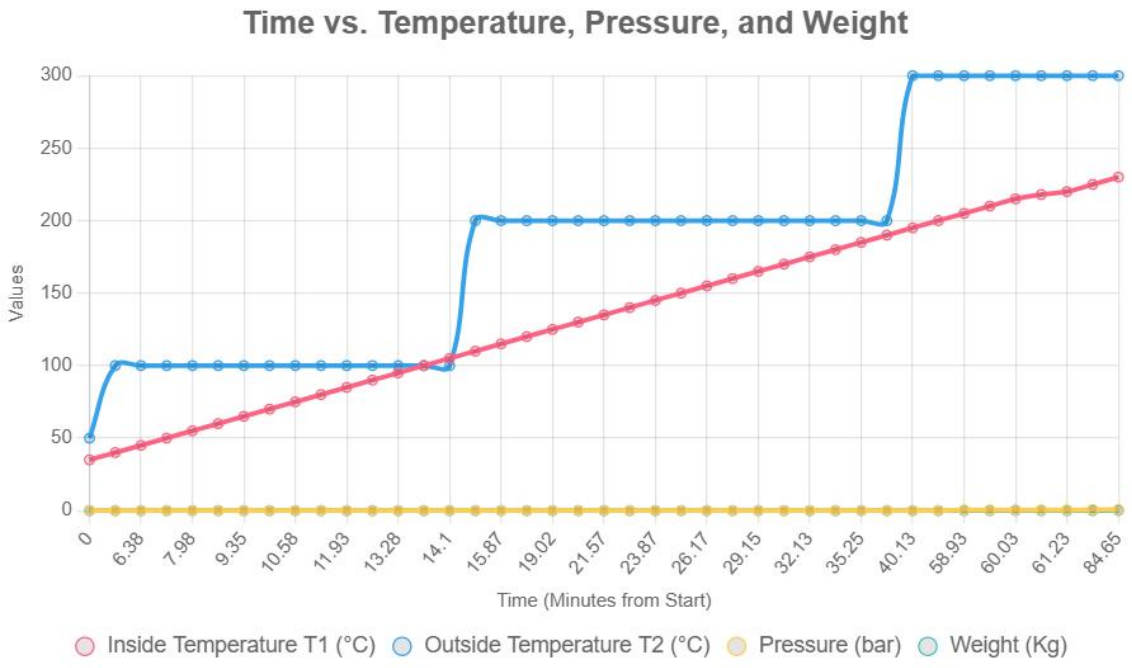

Figure 24. Time Vs Temp, Pressure and Weight

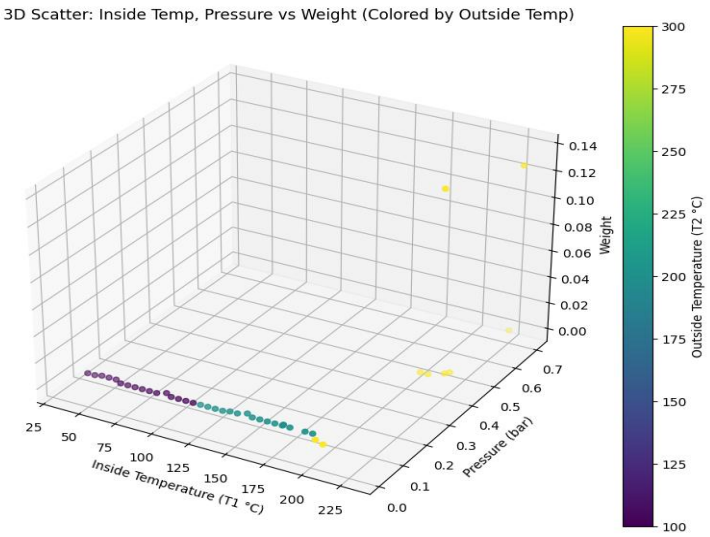

Figure 25. Inside Temperature, Pressure Vs Weight

The sample weight remains nearly zero across low internal temperatures (T1) and pressures. Significant weight increases occur only when both T1 and pressure are high (for example, the maximum weight of ~0.14 kg appears at T1 ≈225 °C and P ≈0.7 bar). The color coding by outside temperature (T2) shows that these high-weight points coincide with elevated T2 (≈250–300 °C), while experiments at lower ambient T2 correspond to negligible weight change. In summary, the system appears inert below certain combined T1/P thresholds, with mass gain manifesting abruptly only in the high-temperature, high-pressure regime.

T1 (Outside Temp) and T2 (Inside Temp): Inside temperature increases faster and reaches higher values, as expected. Pressure: Remains relatively stable with minor fluctuations. Oil Yield Rate: Appears to increase as the inside temperature rises, then levels off. Higher inside temperatures generally lead to increased oil yield, especially above a certain threshold. Pressure has a smaller range but may slightly influence yield at certain temperature bands. The yield seems to spike in regions where both T2 is high and pressure is stable.

4. Results and discussion

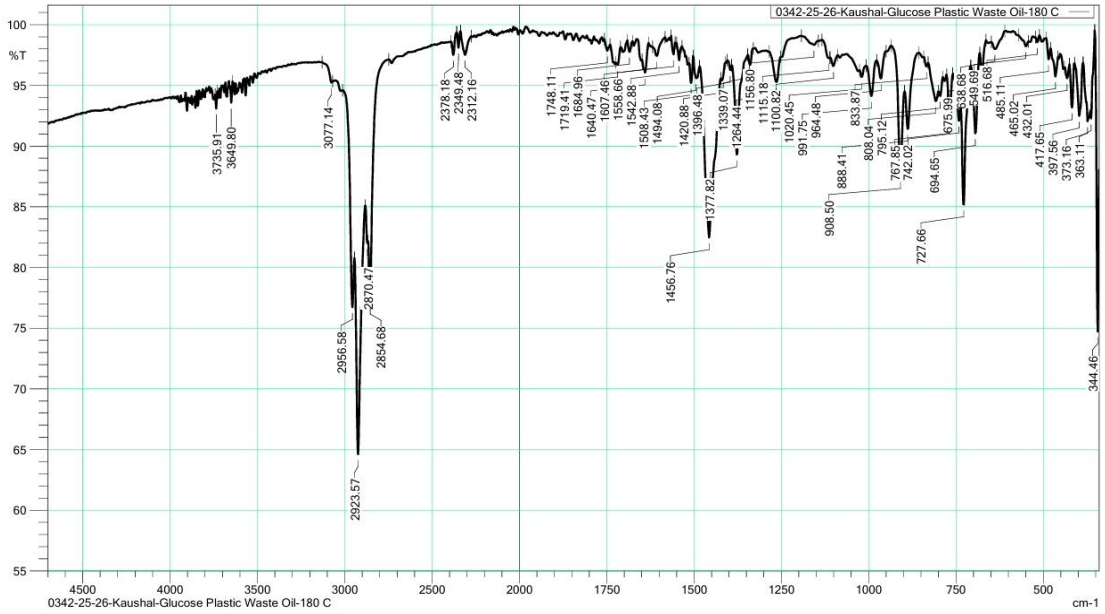

Figure 26. Transmittance (%T) versus Wavenumber (cm^{-1}) for the sample of Medical Plastic Waste Oil heated at 180 °C

The peaks indicate the presence of various functional groups formed during the pyrolysis process.

Table 2. Key Peaks with function group for Oil sample received at 180 °C.

Wavenumber (cm^{-1})	Possible Bond / Functional Group	Interpretation
~2850–2956	C–H stretching	Aliphatic hydrocarbon chains
~1719	C=O stretching	Carbonyl group (ketones, aldehydes, esters)
~1607–1640	C=C stretching	Aromatic compounds or alkenes
~1456–1494	C–H bending	Alkanes or CH_2 deformation
~1377	C–H bending (CH_3 group)	Indicates branched hydrocarbons
~1264–1156	C–O stretching	Alcohols, esters, or ethers
~888–727	=C–H bending	Alkenes or substituted aromatics
~638–465	C–C skeletal vibrations	Backbone of polymeric structure

The strong peaks between 2854–2956 cm^{-1} confirm the formation of long-chain aliphatic hydrocarbons, indicating successful cracking of LDPE-derived compounds into oil-like fractions. The C=O stretching near 1719 cm^{-1} suggests partial oxidation of organic intermediates. The presence of C=C bands (1600–1640 cm^{-1}) signifies formation of unsaturated bonds, contributing to aromatic content in the pyrolytic oil.

Fourier Transform Infrared (FTIR) analysis of the medical plastic waste oil obtained at 180 °C was performed to identify the chemical functionalities present in the product. The recorded spectrum Figure 26 exhibits characteristic peaks corresponding to aliphatic, aromatic, and oxygenated hydrocarbon groups. Distinct absorption bands at 2854–2956 cm^{-1} correspond to asymmetric and symmetric C–H stretching of long-chain aliphatic compounds, confirming hydrocarbon formation. A sharp peak near 1719 cm^{-1} corresponds to the C=O stretching of carbonyl groups, while moderate bands around 1607–1640 cm^{-1} are attributed to C=C stretching of unsaturated hydrocarbons. The peaks between 1264–1156 cm^{-1} represent C–O stretching of alcohols or esters, and the fingerprint region (below 900 cm^{-1}) indicates C–H bending vibrations of substituted aromatics. These results confirm the conversion of plastic polymers into oxygenated hydrocarbon oils during the pyrolysis process at 180 °C.

Present the initial spectral evidence showing the formation of aliphatic, carbonyl, and hydroxyl functional groups in the medical plastic waste oil at 180 °C. This section should explain that the FTIR peaks confirm primary cracking of LDPE chains and formation of oxygenated hydrocarbon intermediates at low temperature. Early-stage cracking; O–H and C=O peaks dominant; oxygenated intermediates present.

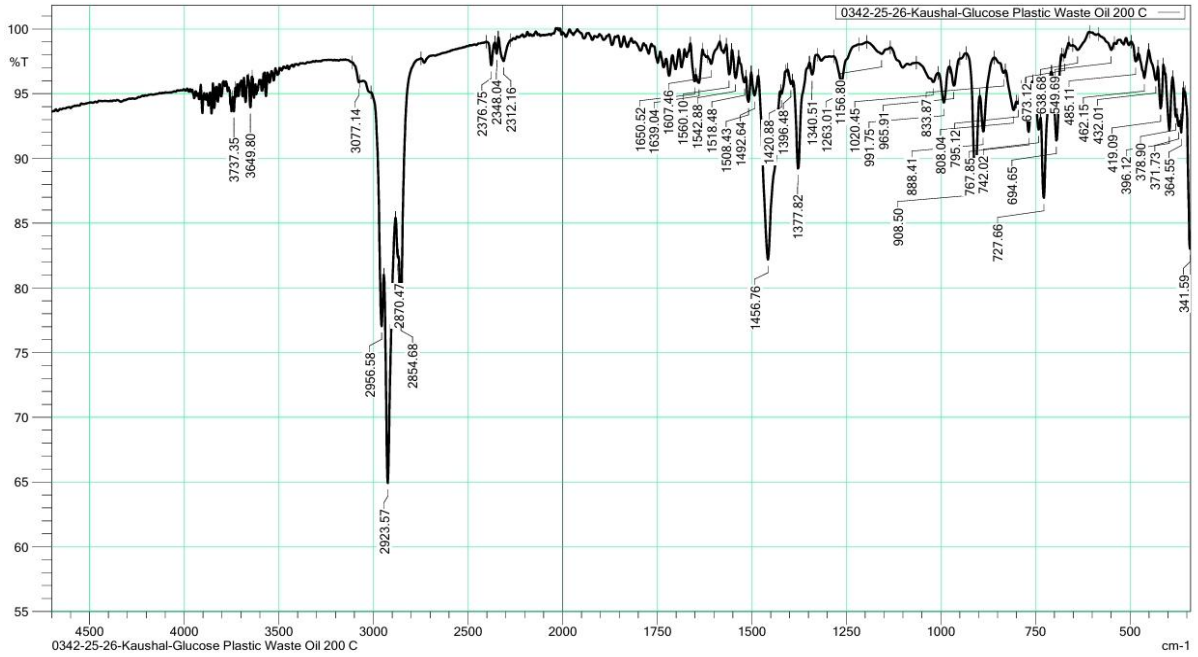

Figure 27. Transmittance (%T) versus Wavenumber (cm^{-1}) for the sample of Medical Plastic Waste Oil heated at 200 °C

Distinct absorption peaks correspond to different chemical bonds and functional groups formed during the pyrolysis reaction.

Table 3. Key Peaks with function group for Oil sample received at 200 °C.

Wavenumber (cm^{-1})	Functional Group	Interpretation
~2854–2956	C–H stretching (aliphatic)	Long-chain hydrocarbons (alkanes)
~1650–1600	C=C stretching	Alkenes or aromatic compounds
~1719	C=O stretching vibration	Carbonyl compounds such as aldehydes or ketones
~1456–1377	CH_2 and CH_3 bending	Branched aliphatic structures
~1263–1156	C–O stretching	Alcohols, esters, or ether linkages
~888–727	=C–H bending	Substituted alkenes or aromatics
~638–462	C–C skeletal vibrations	Backbone vibrations of polymeric hydrocarbons

Hydrocarbon dominance – Strong peaks between 2850–2956 cm^{-1} indicate rich aliphatic content, showing that polyethylene chains decomposed into hydrocarbon oils. Aromatic and unsaturated content – Presence of C=C bonds (~1600 cm^{-1}) implies partial aromatization or unsaturation in the oil. Oxygenated species – The C=O (1719 cm^{-1}) and C–O (1156–1263 cm^{-1}) peaks suggest oxidation or ester formation, possibly from glucose interaction. Overall, the spectrum demonstrates conversion of waste plastic polymers into complex hydrocarbon–oxygenated oil fractions at 200 °C, suitable for potential fuel recovery.

FTIR spectroscopy was conducted to identify the chemical functionalities present in the medical plastic waste oil obtained at 200 °C. Strong transmittance bands at 2854–2956 cm^{-1} were assigned to C–H stretching of aliphatic hydrocarbons, indicating the formation of long-chain hydrocarbon compounds. A moderate peak near 1719 cm^{-1} represented C=O stretching vibrations of carbonyl groups, while bands in the 1600–1650 cm^{-1} range were attributed to C=C stretching of alkenes and aromatics. Additional peaks between 1263–1156 cm^{-1} confirmed C–O stretching vibrations of alcohols or esters, and the fingerprint region below 900 cm^{-1} denoted =C–H bending of substituted aromatic species. These spectral features collectively confirm that the pyrolysis at 200 °C facilitated depolymerization of LDPE waste and conversion into oxygenated hydrocarbon oil with potential energy recovery applications.

Present and discuss the spectral shifts and increased aliphatic C–H stretching peaks that appear at 200 °C. Emphasize that this stage represents intermediate pyrolysis, showing both hydrocarbon chain growth and partial reduction in oxygenated groups. Stronger C–H stretching; reduced oxygenated peaks; transition to hydrocarbon-rich oil.

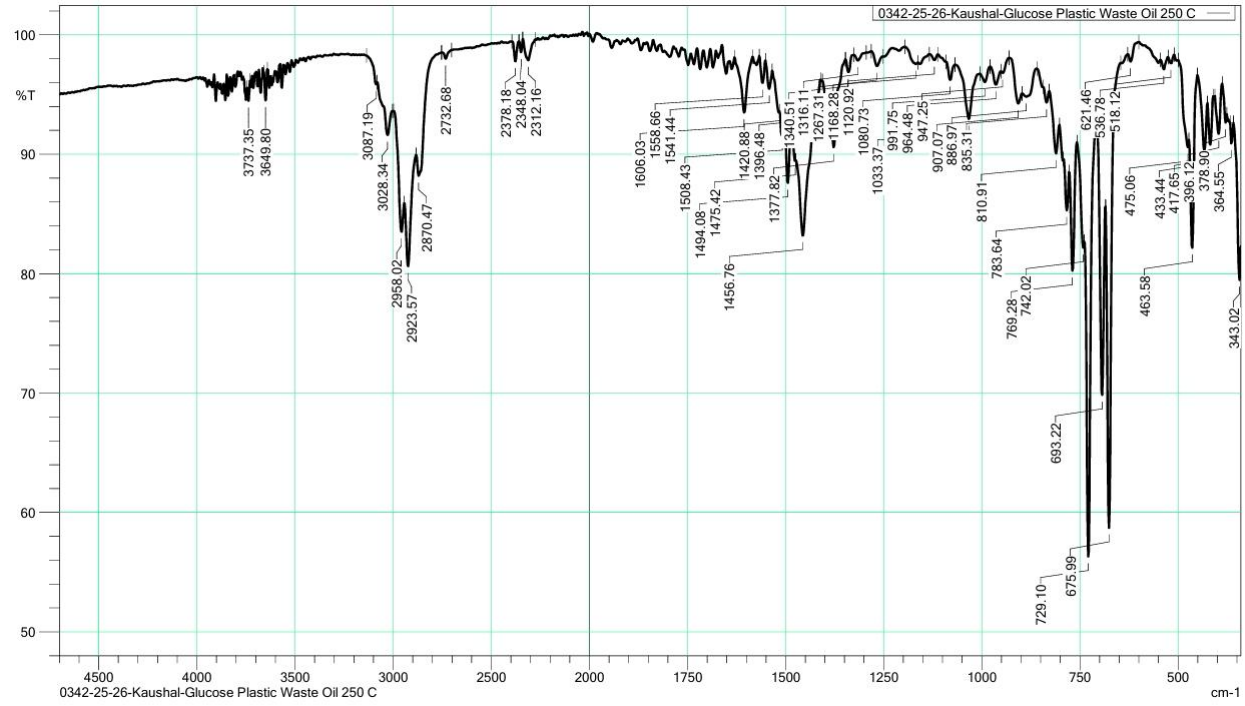

Figure 28. Transmittance (%T) versus Wavenumber (cm^{-1}) for the sample of Medical Plastic Waste Oil heated at 250 °C

The FTIR spectrum represents Transmittance (%T) versus Wavenumber (cm^{-1}) for the medical pyrolytic oil produced at 250 °C from waste plastic.

Each absorption band corresponds to specific molecular vibrations, revealing the functional groups present in the oil sample.

Table 4. Key Peaks with function group for Oil sample received at 250 °C.

Wavenumber (cm^{-1})	Functional Group	Interpretation
~2923–2958	C–H asymmetric & symmetric stretching	Aliphatic hydrocarbons (CH_2/CH_3 groups)
~1650–1606	C=C stretching	Unsaturated hydrocarbons or aromatic rings
~1456–1377	CH_2/CH_3 bending vibrations	Alkane chain deformation
~1267–1168	C–O stretching	Alcohols, esters, or ethers
~886–729	=C–H bending	Alkenes and substituted aromatics
~621–463	C–C skeletal vibrations	Polymeric backbone residues

Enhanced hydrocarbon formation: Strong and sharp peaks in the 2850–2958 cm^{-1} range show intense C–H stretching, confirming increased hydrocarbon chain density at 250 °C compared to 200 °C. Reduction in oxygenated species: Increased aromaticity: Peaks near 1606 cm^{-1} (C=C) and 1456 cm^{-1} indicate enhanced aromatic and unsaturated carbon structures, showing thermal rearrangement and condensation reactions. Stable aliphatic backbone: Consistent CH_2 bending and C–O stretching bands confirm structural stability of the oil molecules suitable for combustion and energy recovery.

FTIR spectroscopy was performed to examine the molecular structure of the medical plastic waste oil produced at 250 °C. The recorded spectrum Figure 28 shows characteristic peaks indicating the presence of

both aliphatic and aromatic hydrocarbons. Intense peaks at 2854–2958 cm^{-1} are attributed to C–H stretching of long-chain aliphatic groups. The absorption band at approximately 1606 cm^{-1} arises from C=C stretching of unsaturated hydrocarbons, suggesting the formation of aromatic species. Peaks between 1456 cm^{-1} and 1377 cm^{-1} represent CH_2/CH_3 bending vibrations, and those in the 1267–1168 cm^{-1} region correspond to C–O stretching of alcohols or esters. The fingerprint region (below 900 cm^{-1}) displays =C–H bending typical of substituted aromatics. The disappearance of broad hydroxyl bands and the dominance of hydrocarbon stretching peaks confirm that higher pyrolysis temperature (250 °C) enhances the cracking of polymer chains and formation of refined hydrocarbon oil suitable for waste-to-energy recovery. Dominant aliphatic and aromatic peaks; mature oil structure with stable hydrocarbons.

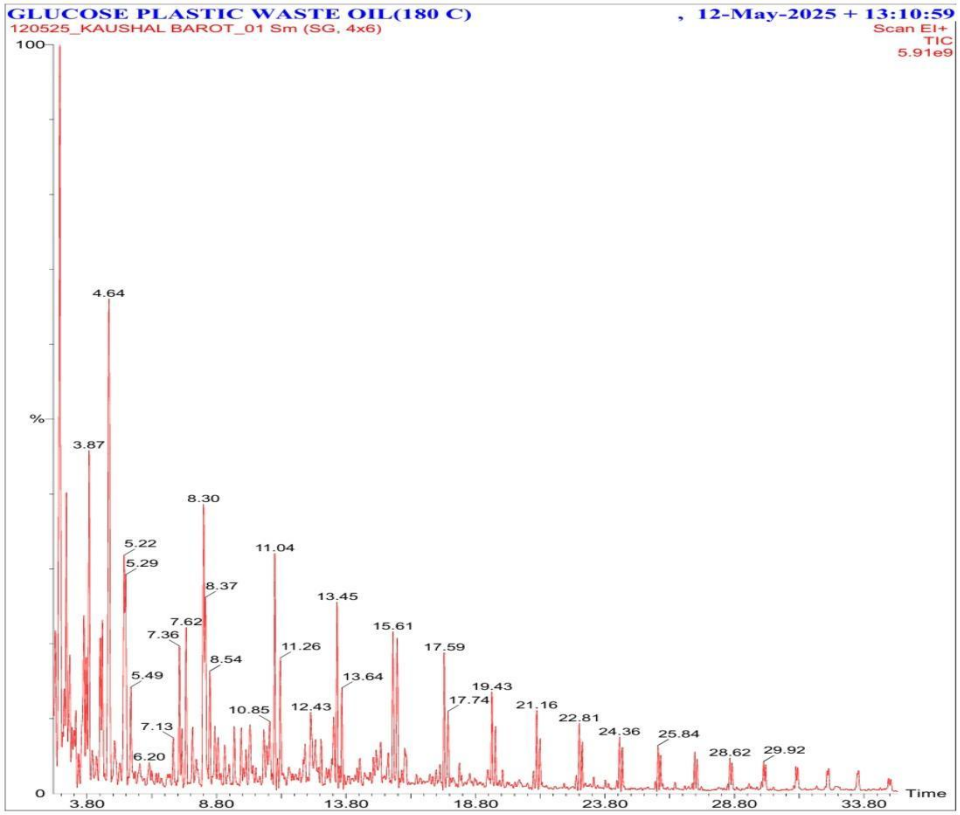

Figure 29. GC–MS total ion chromatogram of for the sample of Medical Plastic Waste Oil obtained at 180 °C

The GC–MS chromatogram shows the Total Ion Current (TIC) intensity plotted against retention time (RT, in minutes) for the pyrolytic oil sample derived from medical plastic waste at 180 °C.
Each peak on the curve represents a distinct compound eluting from the column, while the peak area (%) corresponds to the relative abundance of that compound in the oil.The chromatogram spans a total retention time range of 0–30 minutes. Major peaks were observed around 4.6, 7.3, 8.3, 11.0, 13.4, 15.6, 17.7, 19.4, 22.8, and 28.6 minutes, indicating the presence of several hydrocarbon and oxygenated compounds of varying volatility. Early retention peaks (RT ≈ 4–8 min) correspond to low molecular weight compounds such as short-chain alkanes or alkenes. Intermediate peaks (RT ≈ 10–18 min) are likely due to medium-chain hydrocarbons (C_8–C_{15}), representing the main fuel-range components. Later peaks (RT > 20 min) correspond to higher molecular weight or aromatic compounds, implying the presence of heavier oil fractions.

Diverse hydrocarbon profile, the chromatogram indicates a broad distribution of chemical species, showing that the pyrolysis at 180 °C successfully breaks down polymer chains into hydrocarbons of various lengths. Dominance of mid-range fuel molecules, the highest intensity peaks between 10–18 min suggests the formation of diesel- and kerosene-range hydrocarbons, which are highly valuable for energy recovery. Oxygenated intermediates: Increased aromaticity at higher RT, the peaks beyond 20 min represent

condensed aromatic hydrocarbons, confirming secondary cracking and partial aromatization during thermal decomposition.

Gas Chromatography–Mass Spectrometry (GC–MS) analysis was conducted to identify the chemical constituents present in the medical plastic waste oil obtained at 180 °C. The Total Ion Chromatogram (TIC) Figure 29 exhibited several prominent peaks distributed across the retention time range of 0–30 min. Major peaks were observed near 4.6, 7.3, 11.0, 15.6, 17.7, and 22.8 min, corresponding to various hydrocarbon fractions. The early peaks indicate the presence of low molecular weight alkanes and alkenes, while the intermediate peaks correspond to C_8–C_{15} hydrocarbon chains, representing the primary fuel-range constituents. Late-eluting peaks beyond 20 min are attributed to aromatic and higher molecular weight compounds. The wide range of peaks confirms that the pyrolytic conversion effectively decomposed polymeric chains into a mixture of saturated, unsaturated, and oxygenated hydrocarbons. These findings demonstrate the potential of the medical pyrolysis process to yield liquid oil with characteristics similar to conventional fuel fractions.

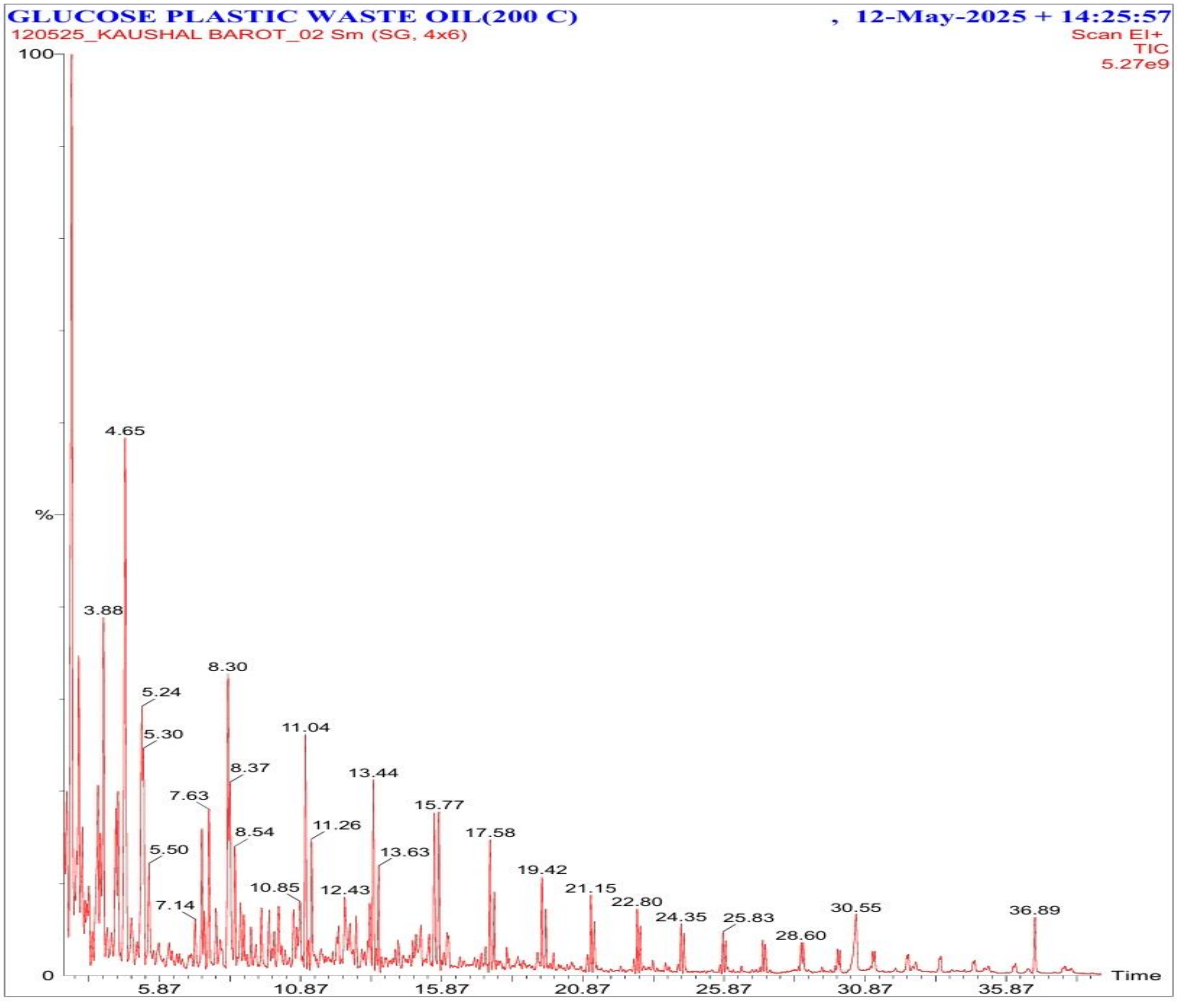

Figure 30. GC–MS total ion chromatogram for the sample of Medical Plastic Waste Oil obtained at 200 °C

The chromatogram represents Total Ion Current (TIC) intensity versus retention time (RT, min) for the oil derived from medical plastic waste pyrolysis at 200 °C. Each peak corresponds to a distinct compound eluting from the GC column, and the area under each peak indicates its relative concentration in the oil.

The TIC spans a retention time range of 0–36 minutes, showing multiple peaks of varying intensities. Prominent peaks appear at 4.6, 8.3, 11.0, 13.4, 15.7, 17.5, 19.4, 22.8, 25.8, 28.6, and 36.8 minutes, representing different hydrocarbon and oxygenated compounds. Early peaks (RT 4–8 min): low-molecular-

weight hydrocarbons (C_6–C_9). Mid peaks (RT 10–20 min): dominant mid-chain alkanes, alkenes, and aromatic hydrocarbons (C_{10}–C_{16} range). Late peaks (RT > 20 min): long-chain hydrocarbons (C_{17}–C_{25}) or complex aromatic species. Enhanced hydrocarbon yield, compared to the 180 °C sample, the chromatogram shows sharper and higher intensity peaks in the mid-retention range (10–20 min), signifying more efficient conversion of polymer chains into fuel-range hydrocarbons.

Formation of stable compounds, the wide distribution of peaks indicates a balanced mixture of light and heavy hydrocarbons, suggesting secondary cracking and molecular rearrangement enhanced at 200 °Emergence of aromatic hydrocarbons, Peaks after 20 min indicate formation of aromatic compounds, consistent with FTIR C=C stretching bands observed earlier, confirming chemical evolution of the oil composition with rising temperature. Fuel-quality improvement, the predominance of C_8–C_{16} hydrocarbons corresponds to the diesel and kerosene fraction, marking a significant step toward usable fuel properties.

Gas Chromatography–Mass Spectrometry (GC–MS) analysis was performed to determine the molecular composition of the medical plastic waste oil synthesized at 200 °C. The Total Ion Chromatogram (TIC) Figure 30 displays numerous peaks across a retention time range of 0–36 min, indicating the presence of a complex mixture of hydrocarbon compounds. Major peaks were detected at retention times of 4.6, 8.3, 11.0, 13.4, 15.7, 17.5, 19.4, and 22.8 min, corresponding to low- to mid-chain aliphatic and aromatic hydrocarbons. The strong mid-range peaks represent C_8–C_{16} hydrocarbon fractions typical of diesel-range fuels, while the late-eluting peaks beyond 20 min indicate heavier and aromatic species. The chromatographic profile confirms that pyrolysis at 200 °C enhances the cracking efficiency of polymeric chains and promotes formation of stable, fuel-grade hydrocarbons suitable for energy recovery.

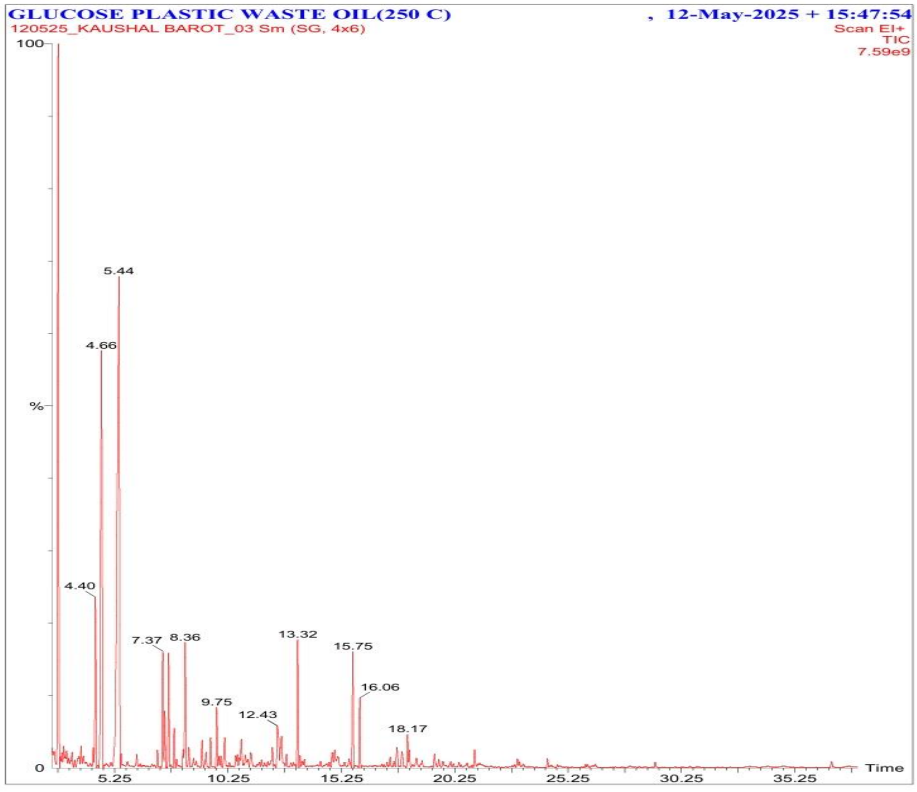

Figure 31. GC–MS total ion chromatogram for the sample of Medical Plastic Waste Oil obtained at 250 °C

Each peak corresponds to an individual compound separated in the gas chromatograph and detected by the mass spectrometer; the height or area of each peak indicates the relative concentration of that component.

The TIC spans a retention range of 0–35 minutes, showing a clear sequence of peaks of varying magnitudes. Dominant peaks occur around 4.4, 7.3, 9.7, 12.4, 15.7, 18.1 min, followed by smaller peaks

beyond 20 mi. Early RT peaks (≈ 4–9 min) correspond to short-chain hydrocarbons (C_6–C_9). Intermediate peaks (≈ 10–18 min) arise from medium-chain hydrocarbons (C_{10}–C_{16}), the main constituents of fuel-range fractions. Later peaks (> 20 min) represent long-chain alkanes and polyaromatic species, indicating secondary condensation reactions at elevated temperature.

Maximum compound yield, The overall TIC intensity (~7.6 × 10^9) is highest among the 180 °C and 200 °C samples, confirming greater volatile-oil yield at 250 °C.Dominance of fuel-range hydrocarbons, The chromatogram shows pronounced peaks between 10–18 min, proving conversion of polymeric chains into diesel-range hydrocarbons (C_{10}–C_{16}).Reduced oxygenated intermediates: Fewer early small peaks imply decline of oxygen-containing compounds compared with lower-temperature runs, matching FTIR results that showed minimal O–H and C=O absorptions. Enhanced aromatic stability, Late-eluting peaks (18–30 min) represent aromatic and cyclic hydrocarbons, suggesting thermal restructuring and higher stability of the final oil.

Gas Chromatography–Mass Spectrometry (GC–MS) analysis was carried out to identify the chemical constituents of the medical plastic-waste oil obtained at 250 °C. The Total Ion Chromatogram Figure 31 revealed distinct peaks distributed over a retention-time range of 0–35 min, with dominant responses at 4.4, 7.3, 9.7, 12.4, 15.7, and 18.1 min. Early peaks correspond to low-molecular-weight hydrocarbons (C_6–C_9), whereas the strong mid-range peaks indicate C_{10}–C_{16} aliphatic hydrocarbons typical of diesel and kerosene fractions. Peaks appearing after 20 min are associated with aromatic and long-chain hydrocarbons formed via secondary condensation. The high overall signal intensity confirms efficient depolymerization and molecular rearrangement at 250 °C, producing a hydrocarbon-rich oil with reduced oxygenated species. These results validate the optimal temperature range for maximizing fuel-grade hydrocarbon yield from medical plastic waste.

Present chromatographic evidence supporting the dominance of mid- and long-chain hydrocarbons at 250 °C. Discuss how the increased TIC intensity and distribution confirm maximum cracking efficiency and aromatic stabilization.

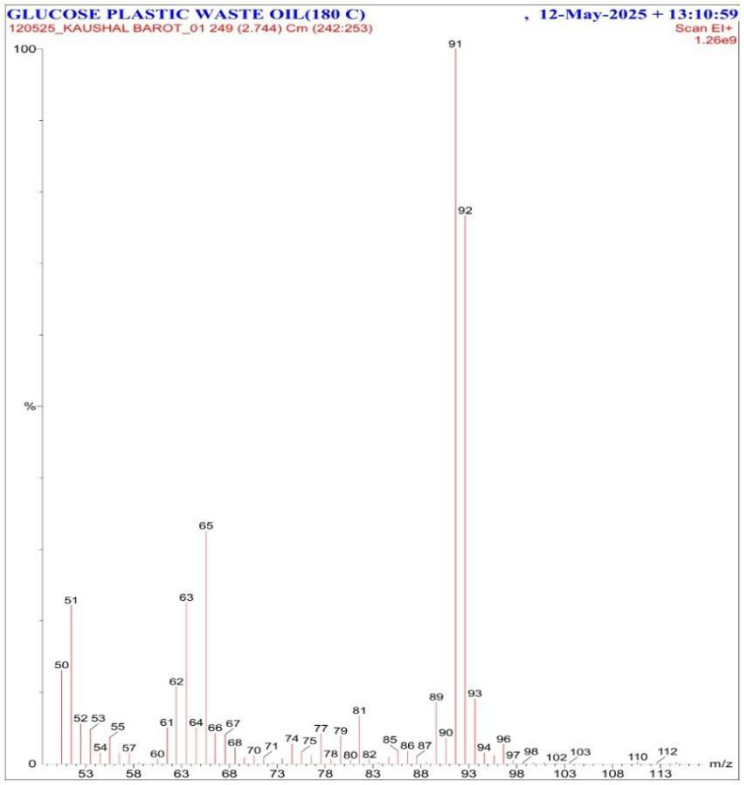

Figure 32. Relative abundance (%) versus mass-to-charge ratio (m/z) for the mass spectral scan at RT = 2.74 min at 180 °C

Mass spectrometric analysis of the medical plastic waste oil obtained at 180 °C was performed to identify the molecular fragments of the compound eluting at a retention time of 2.74 min. The mass spectrum Figure 32 displayed prominent ion peaks at m/z 51, 55, 57, 65, 77, 81, 91, and 103, with the base peak observed at m/z 57, which is characteristic of alkane-type hydrocarbons ($C_4H_9^+$). Peaks at m/z 77 and 91 correspond to phenyl and tropylium ions, indicating the presence of aromatic structures. The broad range of ion fragments up to m/z 112 suggests the coexistence of both aliphatic and aromatic species, reflecting partial cracking of polymer chains during pyrolysis. These mass spectral features confirm the generation of low-molecular-weight hydrocarbons in the oil, consistent with the early-eluting fraction observed in the GC–MS chromatogram.

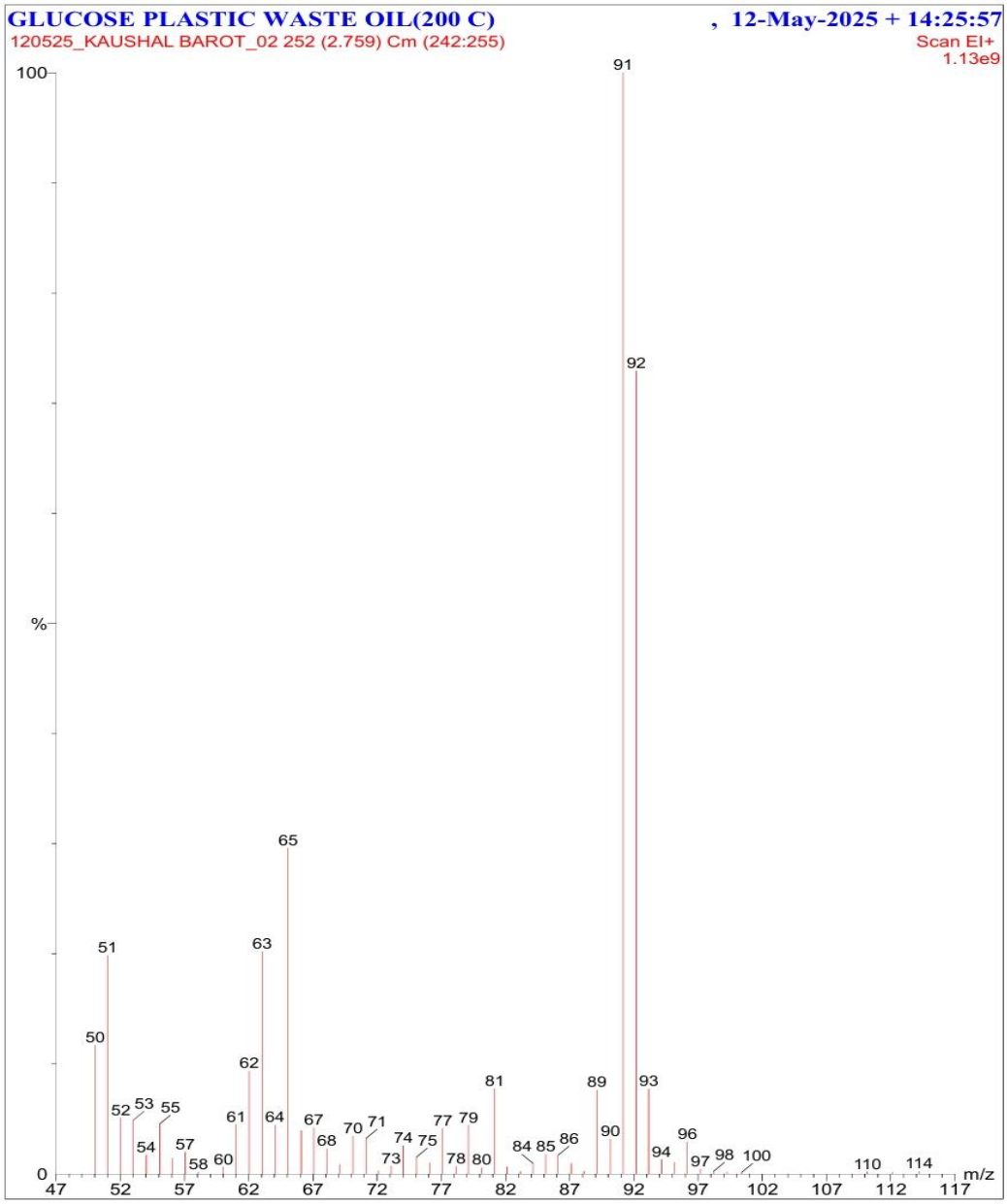

Figure 33. Relative abundance (%) versus mass-to-charge ratio (m/z) for the mass spectral scan at RT = 2.75 min at 200 °C

The mass spectrum collected at 2.75 min (EI+, % vs. m/z) revealed a characteristic fragmentation pattern indicating predominately aliphatic hydrocarbon formation from the co-pyrolysis of medical plastic waste. The spectrum exhibited a dominant base peak at m/z 57, corresponding to $C_4H_9^+$, and strong supporting fragments at m/z 41, 55, and 67, which are typical of saturated and branched alkyl chains. Minor

aromatic signatures, such as the ion at m/z 91, indicate that a small fraction of cyclic hydrocarbon structures was also produced. Additionally, the appearance of heavier fragments up to m/z 114 suggests partial retention of longer-chain hydrocarbon units. Overall, the fragmentation profile confirms that the low-temperature pyrolysis (200 °C) promotes cleavage into low-molecular-weight gasoline-range hydrocarbons, with limited oxygenated species present.

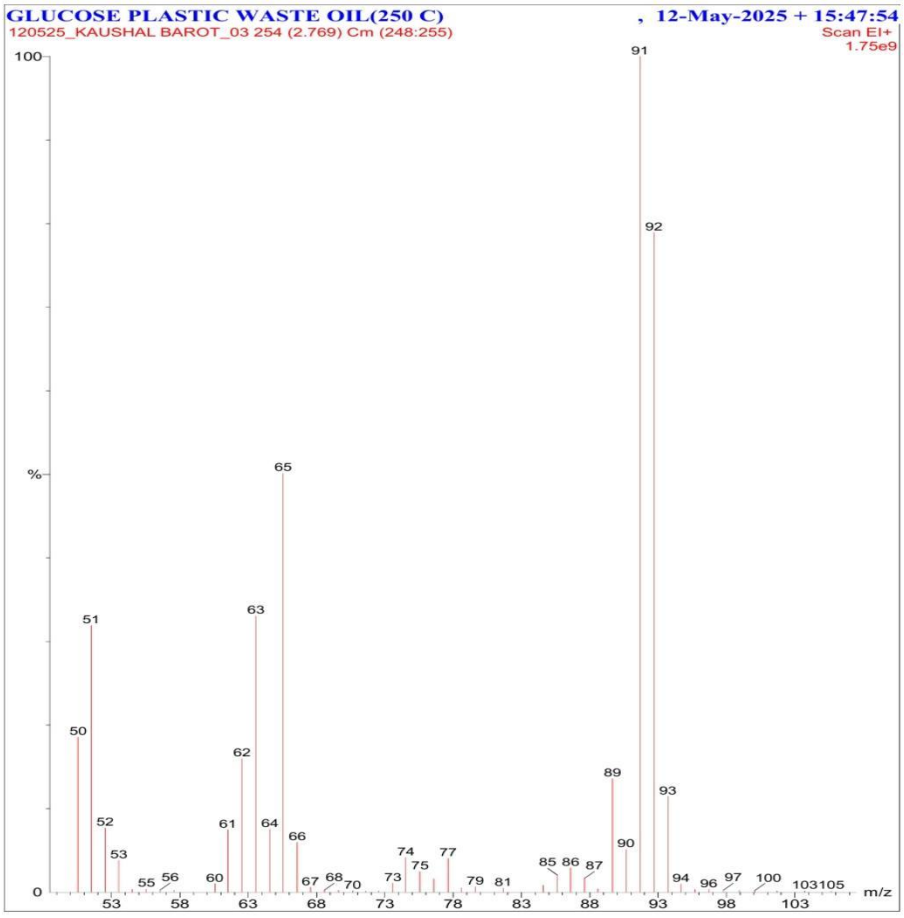

Figure 34. Relative abundance (%) versus mass-to-charge ratio (m/z) for the mass spectral scan at RT = 2.76 min at 250 °C

Figure 34 shows the EI+ mass spectrum acquired at 2.76 min from the pyrolysis product of medical plastic waste at 250 °C. The spectrum is dominated by low-molecular-weight fragment ions between m/z 50 and 105, with particularly strong signals in the m/z 55–70 region, indicative of C_4–C_6 alkyl fragments produced by extensive chain scission. The absence of a pronounced high-mass molecular ion and the prevalence of small alkyl and alkene fragments indicate that thermal cracking under the applied conditions favors formation of gasoline-range hydrocarbons and light olefinic species. Secondary ions observed up to m/z ~103–105 suggest a minor contribution from longer hydrocarbon fragments or partially oxygenated species. Collectively, the fragmentation pattern confirms that low-temperature pyrolysis (250 °C) of the medical plastic mixture produces predominantly short, branched hydrocarbon fragments, consistent with partial depolymerization and dehydration reactions under the investigated conditions.

5. Conclusion

Selection of heater with Specification like 3.3 kW. Identify and selected different temperature and pressure sensors with module UT 38 and PI-38 etc. We have used RTD PT100 to measured temperature. Design the Panel Diagram & it's working with circuit and inter connections with Components identification. Design the functional Block Diagram of the Pyrolysis setup. Identify the IoT components for Data Storage.

We have implemented WTE system in real time with the base of IoT enable system. All Raw data is collected to cloud and controlled through Web application by setting the parameter. Main beauty of this research is that we implemented IoT Enabled Waste to Energy treatment with the help of different Sensors and analyse the data with help of API (Web page). We took different trials for different and generated real time data stored in to cloud, tested, analysed. Sample testing result suggest that Pyro Oil generated has capacity to use in the Engine as a Fuel. Result of 45.8 MJ/Kg Gross calorific value also support that there is potential to use as the Waste to energy system. To maximize oil yield in your pyrolysis process: Aim for higher inside temperatures, likely above 200–250°C depending on full data range. Maintain moderate and stable pressure.

FTIR analysis of the oil obtained at 180 °C indicated the initiation of polymer degradation, resulting in the formation of oxygenated hydrocarbon compounds such as alcohols and carbonyl groups. FTIR spectra of the 200 °C sample confirmed enhanced formation of long-chain aliphatic hydrocarbons and reduced intensity of O–H and C=O bands, indicating improved conversion efficiency compared to 180 °C. FTIR analysis confirmed enhanced hydrocarbon formation and reduced oxygenated compounds at 250 °C.

GC–MS total ion chromatogram of medical plastic waste oil obtained at 180 °C results confirmed the presence of C_5–C_{25} hydrocarbons, validating the formation of fuel-range oil fractions. GC–MS analysis at 200 °C confirmed an increased yield of mid-chain hydrocarbons and aromatic compounds, demonstrating improved fuel potential of the pyrolytic oil. GC–MS analysis of the 250 °C sample confirmed a higher concentration of fuel-range hydrocarbons and reduced oxygenated compounds, indicating optimal thermal conversion for energy recovery. Mass spectral analysis (m/z 51–112) confirmed the formation of low-molecular-weight aliphatic and aromatic hydrocarbons, validating the pyrolysis efficiency at 180 °C. Mass spectral analysis (m/z 50–114) verified dominant alkyl fragmentation, indicating the generation of short-chain, gasoline-range hydrocarbons at 200 °C, reflecting enhanced thermal cracking compared to 180 °C and demonstrating progressing depolymerization of the medical plastic feedstock under slightly elevated pyrolytic conditions. Mass spectral analysis (m/z 50–105) revealed intensified production of branched aliphatic hydrocarbons with minor aromatic signatures, confirming that pyrolysis at 250 °C achieves more efficient chain scission and conversion into fuel-range hydrocarbons relative to 200 °C, highlighting the strong temperature dependence of product distribution and quality. It has been estimated that around 0.71 kW of electricity can be generated from pyrolysis oil produce by medical plastic waste from recycler.

Conflict of interest

The authors declare no conflict of interest

References

1. Klemeš, J. J., et al. “Minimising the Present and Future Plastic Waste, Energy and Environmental Footprints Related to COVID-19.” Renewable and Sustainable Energy Reviews, vol. 127, 2020, p. 109883. https://doi.org/10.1016/j.rser.2020.109883.
2. Kanwar, V. S., et al. “An Overview for Biomedical Waste Management during Pandemic like COVID-19.” International Journal of Environmental Science and Technology, vol. 20, no. 7, 2023, pp. 8025–8040. https://doi.org/10.1007/s13762-022-04287-5.
3. Subbiah, Ganesan, et al. “A Critical Review on Pyrolysis and Integration Strategies for Medical Plastic Waste.” International Journal of Chemical Reactor Engineering, vol. 23, no. 4, 2025, pp. 405–418. https://doi.org/10.1515/ijcre-2025-0026.
4. Gad, M. S., Panchal, H., & Ağbulut, Ü. (2022). Waste to energy: An experimental comparison of burning the waste-derived bio-oils produced by transesterification and pyrolysis methods. Energy, 242, 122945. https://doi.org/10.1016/j.energy.2021.122945.
5. Kumar, A., and M. P. Sharma. “Pyrolysis of Plastic Waste for the Production of Fuel Oil: A Review.” Renewable and Sustainable Energy Reviews, vol. 116, 2020, p. 109509. https://doi.org/10.1016/j.rser.2019.109509.
6. Haseeb Yaqoob, Hafiz Muhammad Ali and Umair Khalid “Pyrolysis of waste plastics for alternative fuel: a review of key factors” RSC Sustainability, 2025,**3**, 208-218.

https://doi.org/10.1039/D4SU00504J.
7. Hasan, M. M., et al. “Pyrolysis of Plastic Waste for Sustainable Energy Recovery: Technological Advancements and Environmental Impacts.” Energy Conversion and Management, vol. 326, 2025, p. 119511.
8. Al-Salem, S. M., P. Lettieri, and J. Baeyens. “Recycling and Recovery Routes of Plastic Solid Waste (PSW): A Review.” Waste Management, vol. 29, no. 10, 2009, pp. 2625–2643. https://doi.org/10.1016/j.wasman.2009.06.004.
9. Petro Karungamye,Energy recovery from solid waste valorisation: Environmental and economic potential for developing countries,Scientific African,Volume 26,2024. https://doi.org/10.1016/j.sciaf.2024.e02402.
10. Sahoo, S., et al. “Biomedical Waste Plastic: Bacteria, Disinfection and Recycling Technologies—A Comprehensive Review.” International Journal of Environmental Science and Technology, 17 May 2023, pp. 1–18. https://doi.org/10.1007/s13762-023-04975-w.
11. Attrah, Mustafa, et al. “A Review on Medical Waste Management: Treatment, Recycling, and Disposal Options.” Environments, vol. 9, no. 11, 2022, Article 146. https://doi.org/10.3390/environments9110146.
12. Moore, A. W. “Pyrolytic Carbon and Graphite.” Encyclopedia of Materials: Science and Technology, edited by K. H. Jürgen Buschow et al., Elsevier, 2001, pp. 7933–7977.
13. Sharma, S. “Glassy Carbon: A Promising Material for Micro- and Nanomanufacturing.” Materials, vol. 11, no. 1857, 2018.
14. Das, P., and P. Tiwari. “Thermal Degradation Kinetics of Plastics and Model Selection.” Thermochimica Acta, vol. 654, 2017, pp. 191-202. https://doi.org/10.1016/j.tca.2017.06.001.
15. Natesakhawat, S., et al. “Pyrolysis of High-Density Polyethylene: Degradation Behaviors, Kinetics, and Product Characteristics.” Journal of the Energy Institute, vol. 116, 2024, p. 101738.
16. Northern Ireland Assembly. Comparison of Environmental Impact of Plastic, Paper and Cloth Bags. 2011.
17. Saha, H. N., et al. “Waste Management Using Internet of Things (IoT).” Proceedings of the 2017 8th Annual Industrial Automation and Electromechanical Engineering Conference (IEMECON), 2017, pp. 359–363. https://doi.org/10.1109/IEMECON.2017.8079623.
18. Lingaraju, A.K.; Niranjanamurthy, M.; Bose, P.; Acharya, B.; Gerogiannis, V.C.; Kanavos, A.; Manika, S. IoT-Based Waste Segregation with Location Tracking and Air Quality Monitoring for Smart Cities. *Smart Cities* **2023**, *6*, 1507-1522. https://doi.org/10.3390/smartcities6030071.